

Review

Research Progress and Prospect of Condition Assessment Techniques for Oil–Paper Insulation Used in Power Systems: A Review

Zaijun Jiang ¹, Xin Li ², Heng Zhang ¹ , Enze Zhang ¹ , Chuying Liu ¹, Xianhao Fan ^{3,*} and Jiefeng Liu ¹ 

¹ Guangxi Key Laboratory of Power System Optimization and Energy Technology, Guangxi University, Nanning 530004, China; 2112301032@st.gxu.edu.cn (Z.J.); hengzhang_gxu@163.com (H.Z.); enze_zhang1@163.com (E.Z.); 2012392050@st.gxu.edu.cn (C.L.); jiefengliu2018@gxu.edu.cn (J.L.)

² State Grid Sichuan Electric Power Company Ultra High Voltage Branch, Chengdu 610041, China; daisylixin@163.com

³ Department of Electrical Engineering, Tsinghua University, Beijing 100084, China

* Correspondence: xianhaofan@tsinghua.edu.cn; Tel.: +86-15577167221

Abstract: Oil–paper insulation is the critical insulation element in the modern power system. Under a harsh operating environment, oil–paper insulation will deteriorate gradually, resulting in electrical accidents. Thus, it is important to evaluate and monitor the insulation state of oil–paper insulation. Firstly, this paper introduces the geometric structure and physical components of oil–paper insulation and shows the main reasons and forms of oil–paper insulation’s degradation. Then, this paper reviews the existing condition assessment techniques for oil–paper insulation, such as the dissolved gas ratio analysis, aging kinetic model, cellulose–water adsorption isotherm, oil–paper moisture balance curve, and dielectric response technique. Additionally, the advantages and limitations of the above condition assessment techniques are discussed. In particular, this paper highlights the dielectric response technique and introduces its evaluation principle in detail: (1) collecting the dielectric response data, (2) extracting the feature parameters from the collected dielectric response data, and (3) establishing the condition assessment models based on the extracted feature parameters and the machine learning techniques. Finally, two full potential studies are proposed, which research hotspots’ oil–paper insulation and the electrical–chemical joint evaluation technique. In summary, this paper concludes the principles, advantages and limitation of the existing condition assessment techniques for oil–paper insulation, and we put forward two potential research avenues.

Keywords: power system; oil–paper insulation; condition assessment; dielectric response technique; machine learning technique



Citation: Jiang, Z.; Li, X.; Zhang, H.; Zhang, E.; Liu, C.; Fan, X.; Liu, J. Research Progress and Prospect of Condition Assessment Techniques for Oil–Paper Insulation Used in Power Systems: A Review. *Energies* **2024**, *17*, 2089. <https://doi.org/10.3390/en17092089>

Academic Editor: Claus Leth Bak

Received: 29 February 2024

Revised: 2 April 2024

Accepted: 17 April 2024

Published: 26 April 2024



Copyright: © 2024 by the authors. Licensee MDPI, Basel, Switzerland. This article is an open access article distributed under the terms and conditions of the Creative Commons Attribution (CC BY) license (<https://creativecommons.org/licenses/by/4.0/>).

1. Introduction

As the most efficient and economical electric transmission method, ultra-high voltage (UHV) transmission has the advantages of long-distance transmission, large capacity, and low energy loss [1]. There are more than 40 types of power equipment operating on the UHV transmission lines to complete the power transmission and conversion tasks, such as power transformers, reactors, UHV gas-insulated switches, and cables [2]. In the practical electrical engineering site, the above power equipment generally operates under extremely severe conditions, such as a high-voltage field, high-temperature field, and strong mechanical stress [3]. Thus, for ensuring the safe and effective operation of the UHV transmission line, it is necessary and significant to monitor the operation state of the above power equipment [4].

The oil–paper insulation system takes the function of insulation, arc extinguishing, geometric isolation, and cooling in various power equipment, such as power transformers, bushings, and cables [5]. Specifically, oil–paper insulation is formed of insulating paper and

insulating oil [6]. In the practical electrical engineering site, the oil–paper insulation system always operates under severe conditions, such as high temperature, high load, and complex electromagnetic fields [7]. Under the synergistic effect of the above factors, the oil–paper insulation system undergoes thermal aging, moisture invasion, mechanical damage, and chemical corrosion [8]. These situations cause a sharp decline in the insulation performance and mechanical properties of the oil–paper insulation, resulting in the breakdown of the power equipment and the collapse of the power system [9]. According to the existing research [10], thermal aging and moisture intrusion are two main factors which cause the degradation of oil–paper insulation. Therefore, it is important to research the aging degree and moisture content of oil–paper insulation.

In order to effectively understand the research trends in the field of oil–paper insulation state assessment in recent years, this paper adopted the bibliometric method to systematically comb through the current research status, research hotspots, and future development trends in the field of oil–paper insulation state assessment. At the same time, based on “oil–paper insulation” and “condition assessment” as keywords, we searched for relevant content references from 2010 to 2023 in the Web of Science database. We found a total of 1962 articles in the Web of Science database, with a total citation count of 19,851 times, and the specific data are recorded in Table 1. Comparing the number of papers and citation counts from 2010 to 2023, the number of publications in the related field has significantly increased, indicating that more and more researchers and institutions are beginning to focus on this field. At the same time, the substantial increase in citation counts indicates that the literature in this field has had a significant impact on subsequent research, receiving widespread attention and usage by researchers. Therefore, the analysis of oil–paper insulation condition assessment technology is of significant importance.

Table 1. Equations between the content of furfural and DP of the insulating paper.

Number	Research Indicator	Detailed Information
1	Keywords	Oil–paper insulation and condition assessment
2	Data source	Web of science
3	Time span	2010–2023
4	Literature type	Article
5	Literature quantity	1962
6	Total citation	19,851

This paper reviews the research progress and prospects of condition assessment techniques for oil–paper insulation. In Section 2, this paper introduces the composition and application of oil–paper insulation. Additionally, the reasoning and mechanisms for oil–paper insulation deterioration are explained. In Section 3, the existing assessment techniques for the aging degree of oil–paper insulation are reviewed. Further, their inadequacies and advantages are introduced and compared. In Section 4, the existing assessment techniques for the moisture content of oil–paper insulation are reviewed and their inadequacies and advantages are introduced and compared. In Section 5, this paper introduces the theories and advantages of the dielectric response technique, which can simultaneously evaluate the aging degree and moisture content of oil–paper insulation. In Section 6, based on the limitations of the existing research, this paper proposes two potential research topics for future work, which focus on hotspots’ oil–paper insulation and the electrical–chemical joint assessment technique. In order to introduce and compare the existing oil–paper insulation condition assessment technologies more intuitively, we have summarized the assessment technologies within the research field and drawn a flowchart of the current state of research on oil–paper insulation condition assessments, as shown in Figure 1. The figure displays nine technologies in the field of oil–paper insulation condition assessments and the corresponding technical defects. Meanwhile, it outlines the technical route of dielectric response technology that can comprehensively assess aging degree and moisture content.

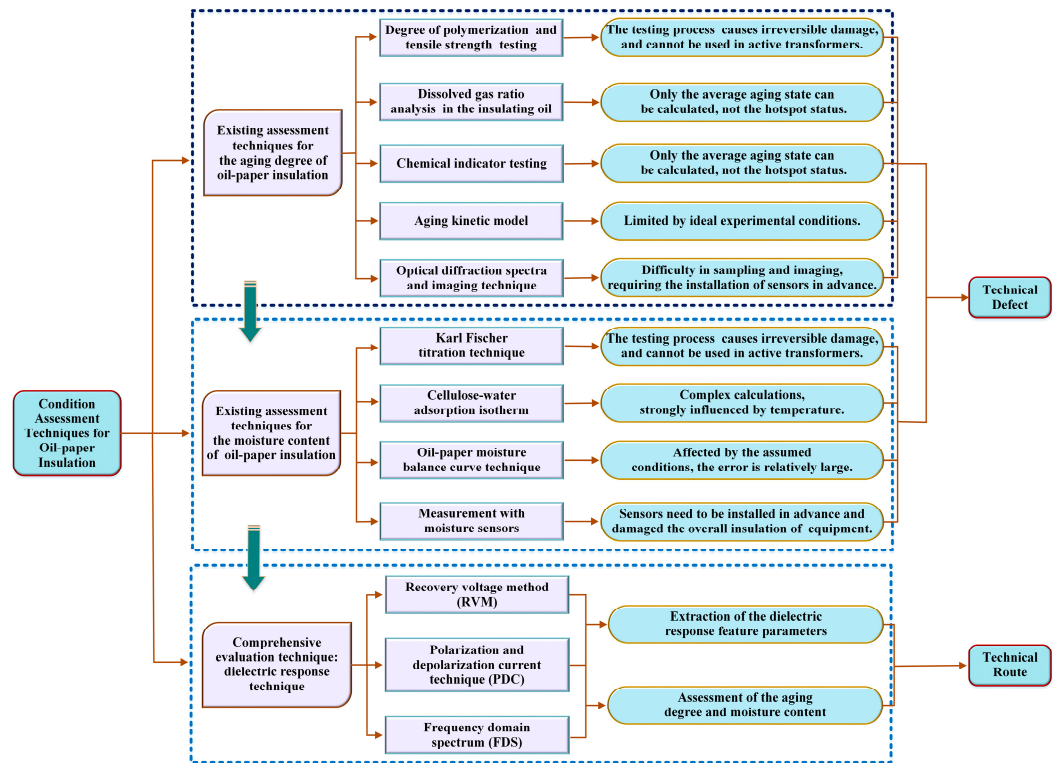


Figure 1. Flowchart of the current status of oil–paper insulation state assessment research.

2. The Background of Condition Assessments for Oil–Paper Insulation

2.1. The Composition of Oil–Paper Insulation

Oil–paper insulation is composed of insulating paper and insulating oil. In the operation of power equipment, the insulating paper plays the role of isolation, support, and insulation [11]. Meanwhile, the insulating oil plays the role of heat dissipation, arc suppression, and insulation. The composite structure of the oil–paper insulation in a power transformer is shown in Figure 2, as a typical example. The physical structure of the insulating paper is fluffy, and there are lots of natural pores existing in the insulating paper [12]. This physical structure leads the insulating paper to absorb the moisture and impurities in the power equipment, resulting in the distortion of the electric field and a reduction in insulation performance. To address this issue, insulating oil has been adopted to fill these pores and prevent the intrusion of moisture and impurities. Therefore, the physical structure of the oil–paper insulation has been improved and the insulation property has been greatly enhanced.

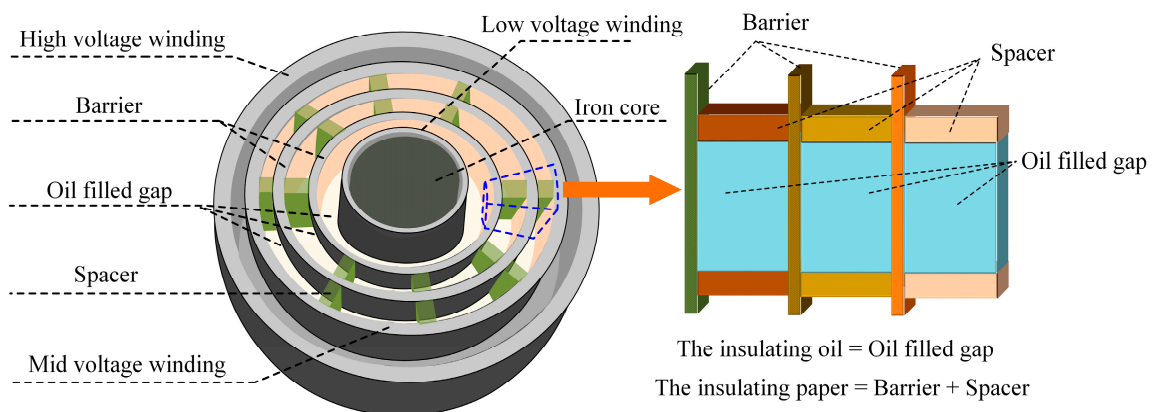


Figure 2. The composite structure of the oil–paper insulation in a power transformer.

2.1.1. Insulating Paper

The insulating paper is prepared by treating wood pulp with unbleached sulfate pulp [13]. The insulating paper is commonly composed of three chain polymer compositions: cellulose (about 90%), hemicellulose (6–7%), and lignin (3–4%). At the macroscopic level, the cellulose chain is composed of β -D-glucose monomers ($C_6H_{12}O_5$) connected by 1,4- β glycosidic bonds. At the microscopic level, the cellulose chain contains multiple asymmetric repeating units (cellulose disaccharides) arranged in series, and there are three hydroxyl groups in the above-repeating unit [14]. Meanwhile, there are lots of hydrogen bonds formed within and between the cellulose chains, which ensure the tight binding of cellulose chains. Thus, insulating paper has the advantages of high mechanical strength, stable chemical properties, and high breakdown strength. The macrostructure of insulating paper and the microstructure of the cellulose chain are shown in Figure 3.

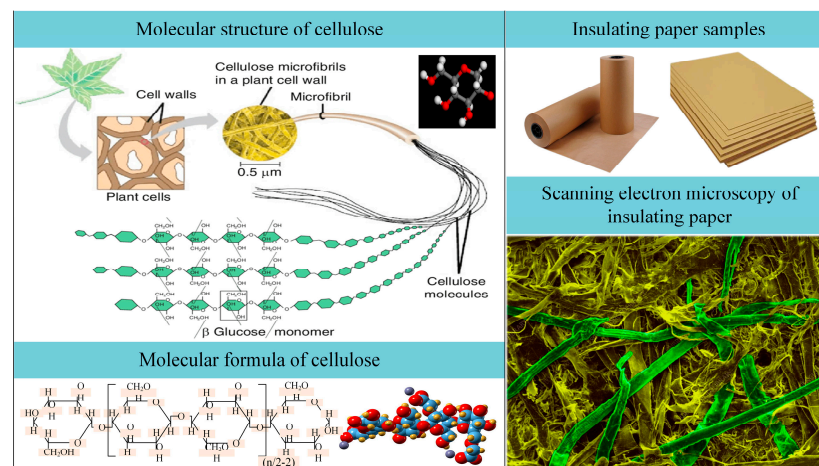


Figure 3. Macrostructure of insulating paper and microstructure of the cellulose chain.

2.1.2. Insulating Oil

Due to the advantages of a low price, strong thermal conductivity, and good insulation performance, mineral oil is widely used as insulating oil in various power equipment. Mineral oil is a refined liquid hydrocarbon mixture, which is prepared by atmospheric and decompression fractionation, solvent extraction, dewaxing, and hydro-refining of crude oil [15]. Mineral oil is commonly odorless and tasteless at low temperatures. In addition, mineral oil is mainly composed of hydrocarbon compounds, which make up more than 95 percent of the oil [16]. The hydrocarbons in mineral oil mainly include alkanes, naphthenic hydrocarbon, and alkyl aromatic hydrocarbon. Insulating oil samples and the molecular structure of their main compounds are shown in Figure 4.

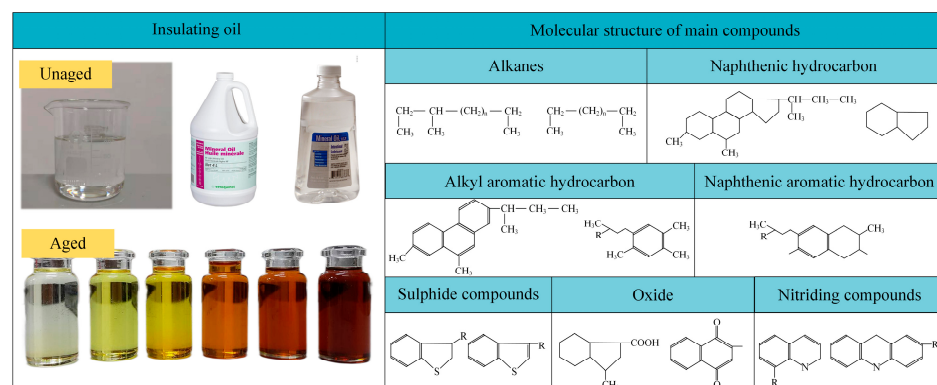


Figure 4. Insulating oil samples and molecular structure of their main compounds.

2.2. The Degradation of Oil–Paper Insulation

Due to the satisfactory insulation performance of oil–paper insulation, it has been widely used in various power equipment as an insulation material [5]. In a practical electrical engineering site, the power equipment mostly operates in complex and severe conditions, such as high voltage, high temperature, and severe dampness. Under these severe operating conditions, the oil–paper insulation suffers various stresses, such as thermal stress, mechanical stress, and electrical stress [8]. With the effect of these stresses, the oil–paper insulation gradually deteriorates, and its insulation performance gradually decreases [9]. According to the existing research [10], the degradation of oil–paper insulation can be divided into temporary deterioration and cumulative deterioration. Cumulative deterioration mainly includes aging and dampness.

2.2.1. Temporary Deterioration

Temporary deterioration is usually caused by instantaneous high-impact current and instantaneous high-impact force [17]. Under the effect of instantaneous high-impact current, the free electrons in oil–paper insulation move extremely quickly, and there is a large amount of kinetic energy accumulated in the oil–paper insulation. The above kinetic energy is enough to destroy the molecular structure of oil–paper insulation, and there are conductive channels produced through the oil–paper insulation. Further, the insulation performance decreases rapidly, resulting in an electric breakdown. Under the instantaneous high-impact force, the oil–paper insulation suffers tremendous mechanical stress, and the physical structure of the insulating paper is destroyed. Further, the insulating paper deforms and cracks, resulting in the failure of the oil–paper insulation [18]. However, temporary deterioration is a phenomenon whereby the insulation's performance decreases dramatically, caused by irregular operation and transient overvoltage. In contrast, cumulative deterioration is the phenomenon whereby the insulation's performance decreases gradually under the long-term influence of various natural stresses.

2.2.2. Cumulative Deterioration: Aging

Under complex and severe operating conditions, oil–paper insulation ages in multiple forms, which include oxidation degradation, pyrolysis, hydrolysis, photochemical cracking, and microbial catalytic degradation. Each aging form has a corresponding aging condition and mechanism [19]. During the above aging processes, the hydrogen bonds within and between the cellulose chains in the insulating paper are gradually broken. Meanwhile, the chemical bonds in the hydrocarbon compounds in the insulating oil are also broken. There are lots of small molecular byproducts generated in the oil–paper insulation during the above aging processes, such as H₂O, CO, CO₂, methanol, ethanol, formic acid, acetic acid, and furfural. Further, the small molecular byproducts that are generated can cause more complex chemical reactions in the oil–paper insulation, such as water molecules that can promote the hydrolysis of the cellulose chains. As a result, the above aging processes reduce the insulation performances and mechanical properties of oil–paper insulation.

2.2.3. Cumulative Deterioration: Dampness

The dampness of oil–paper insulation has two main sources [20], which are moisture invasion and aging reaction. Moisture invasion can be divided into three forms: (1) Some moisture is inevitably retained during the production and installation of power equipment. (2) External moisture enters the oil–paper insulation during the maintenance of power equipment. (3) Due to the fact that power equipment cannot be completely sealed, the moisture from other parts seeps into the oil–paper insulation. The moisture generated by the aging reaction can be divided into two forms: (1) The breakage of the cellulose chain in the insulating paper generates some moisture. (2) The oxidation of the hydrocarbon compounds in the insulating oil generates some moisture. Due to the porous structure of the insulating paper, 99% of the moisture exists in the insulating paper, and only 1% of the moisture diffuses into the insulating oil.

2.3. The Possibility of Electrical Accidents

Electricity is a danger that cannot be ignored in modern life. Although electricity-related accidents do not represent a high proportion of the total number of occupational accidents occurring annually worldwide, they account for a higher proportion of fatalities than any other type of accident. According to the statistics of the Ministry of Labour of Greece, electrical work accidents account for about 1% of total work accidents, and about 24% are fatal [21]. From the perspective of economic loss, electrical accidents not only pose a serious threat to personnel safety but also lead to a series of economic consequences. These accidents can cause damage to expensive equipment, necessitating high costs for repair or replacement, and may also lead to the suspension of production activities, resulting in even greater economic losses. For example, the major blackout in the United States in 2003 affected about 50 million people for several days. It directly impacted multiple industries such as industrial, food, and pharmaceuticals sectors, causing losses of about USD 10 billion.

Therefore, oil–paper insulation as a key component of power systems directly affects the incidence of power accidents. Under the synergistic action of dampness and thermal effects, the oil–paper insulation system undergoes significant aging, resulting in degradation of its insulating properties and even explosions. In the event of a transformer failure or accident, there is a high probability that it will bring life-threatening danger to personal safety. And it will also cause huge maintenance requirements and equipment loss. Under these circumstances, techniques for evaluating the aging state of oil–paper insulation are crucial [22].

3. Techniques for Evaluating the Aging State of Oil–Paper Insulation

3.1. Degree of Polymerization (DP) and Tensile Strength (TS) Testing

According to the existing research [23], the average number of glucose monomers contained in each cellulose chain has been defined as the degree of polymerization (DP) of the insulating paper. Thus, the DP is an effective and intuitive indicator which can reflect the microphysical structure of the cellulose chains in the insulating paper. During the aging process of oil–paper insulation, the cellulose chains in the insulating paper are broken constantly, and the glucose monomers contained in each cellulose chain decrease constantly. Thus, the number of glucose monomers is inversely proportional to the aging time of the insulating paper. Further, the degree of polymerization (DP) can reflect the aging degree of the insulating paper. Specifically, the smaller the DP, the more serious the aging degree of the insulating paper.

In the literature [24], Oomen et al. have proposed viscosity testing as an effective method to obtain the DP of insulating paper. They have also obtained the quantitative relationship between the DP of the insulating paper and its aging degree, in addition to the classification standard of the insulating paper's aging degree, established based on the DP. In actual industrial production, the initial DP of the new insulating paper is generally 1000–1300. Then, the DP decreases to about 900 after drying and oiling. According to the national standard [25], while the DP of the insulating paper is less than 500, the aging degree of the oil–paper insulation reaches the middle level. While the DP of the insulating paper is less than 250, the aging degree of the oil–paper insulation reaches a high level, and the operating life of the oil–paper insulation reaches its end.

The tensile strength (TS) of the insulating paper has been defined as the maximum resistance to uniform plastic deformation [26]. It is a characteristic indicator similar to the DP, which can directly reflect the mechanical strength of the insulating paper. Montsinger et al. have proved that tensile strength is an effective indicator to reflect the aging degree of insulating paper, and they have researched the relationship between the TS of the insulating paper and its aging degree [27]. Specifically, the smaller the TS, the more serious the aging degree of the insulating paper. Meanwhile, they have proposed that the operating life of oil–paper insulation has reached its end when the tensile strength of the insulating paper has reduced to half of the unaged insulating paper.

The testing process of the tensile strength (TS) and degree of polymerization (DP) of the insulating paper is shown in Figure 5. However, in a practical electrical engineering site, DP and TS testing require one to obtain insulating paper samples from the operating power equipment, which causes irreparable damage to its oil–paper insulation. In addition, the sampling process requires the power equipment to be offline and the oil–paper insulation to be exposed to the air, which can cause moisture in the environment to enter the oil–paper insulation system. In summary, DP and TS testing are suitable for researching the aging degree of oil–paper insulation, which has been proven under laboratory conditions. Researchers have been unable to research the aging degree of oil–paper insulation in in-service power equipment.

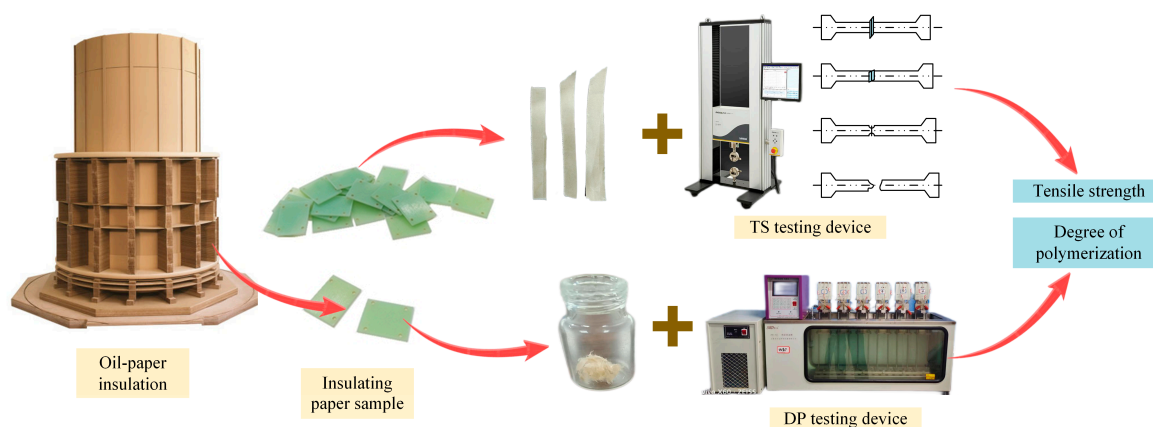


Figure 5. A schematic diagram of DP testing and TS testing.

3.2. Dissolved Gas Ratio Analysis (DGA) in Insulating Oil

During the aging process of oil–paper insulation, the cellulose chains in the insulating paper break down gradually. There are various gaseous compounds (such as hydrogen H_2 , methane CH_4 , ethane C_2H_6 , ethylene C_2H_4 , acetylene C_2H_2 , carbon monoxide CO , and carbon dioxide CO_2) produced and dissolved in insulating oil [28]. According to the IEEE Std C57.104-1991 [29] and IEC 60599-1999 [30] standards, the above gaseous compounds can be separated from the insulating oil with the degassing technology. Then, the content and ratio of the above gaseous compounds can be quantitatively analyzed based on gas chromatography analysis technology.

Rogers et al. have researched the relationship between the aging degree of oil–paper insulation and the content of various gaseous compounds dissolved in the insulating oil [31]. They have proved that the ratio of gaseous compounds (CH_4/H_2 , C_2H_6/CH_4 , C_2H_4/C_2H_6 , and C_2H_2/C_2H_4) can be adopted to evaluate the aging degree of oil–paper insulation. However, C_2H_6/CH_4 is only effective in the limited temperature range. Thus, after removing the C_2H_6/CH_4 , the three-ratio analysis method has been generally accepted in recent years. In addition, with research on carbon and oxygen gaseous compounds, M. Duval et al. have found the following rules [32]:

- (1) $CO_2/CO > 7$: Oil–paper insulation is in the normal operating state.
- (2) $CO_2/CO < 6$: Oil–paper insulation is in the stage of accelerated aging.
- (3) $CO_2/CO < 2$: Oil–paper insulation is at a serious aging degree.

Tamura et al. have proposed a quantitative relationship between the total content of CO and CO_2 dissolved in insulating oil and the residual rate of the insulating paper's DP [33]:

- (1) $CO + CO_2 \approx 1 \text{ mL/g}$: The residual rate of DP is about 50%, and the insulating paper is in the middle aging degree.
- (2) $CO + CO_2 \approx 3 \text{ mL/g}$: The residual rate of DP is about 30%, and the insulating paper is in the serious aging degree.

The production mechanisms of the above gaseous compounds are relatively clear, and the sources of the relevant data are relatively extensive. Thus, dissolved gas ratio analysis (DGA) technology has been widely applied in the condition assessment for oil–paper insulation. In addition, DGA technology can realize the online assessment without interrupting the operation of power equipment. A schematic diagram of the dissolved gas ratio analysis is shown in Figure 6.

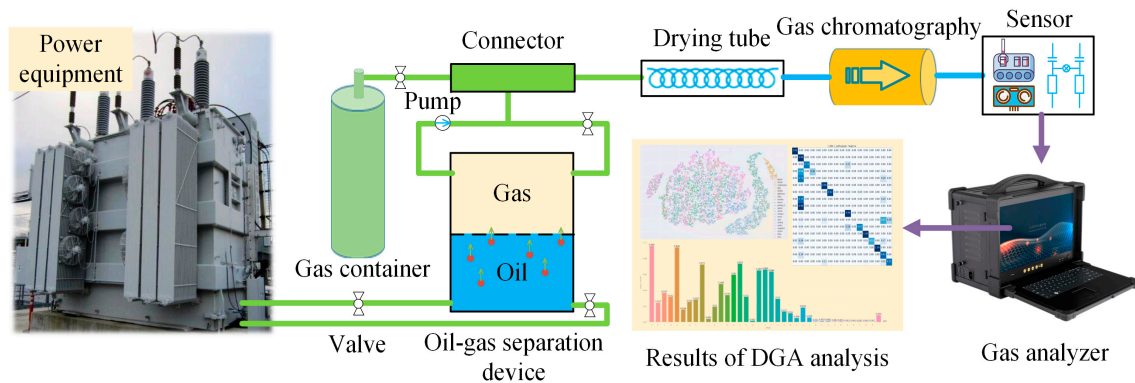


Figure 6. A schematic diagram of dissolved characteristic gas analysis.

However, there are still some limitations existing with DGA technology for the condition assessment for oil–paper insulation [34]:

- (1) Some of the gaseous compounds are lost during the operation of pressure oil filtration and high vacuum oil filtration, which causes a deviation in the evaluation results.
- (2) The oxidative cracking of insulating oil and the aging of insulating paper produce the same gaseous compounds. Thus, DGA technology cannot independently evaluate the aging state of the insulating paper or the insulating oil.
- (3) DGA technology is effective to evaluate the average aging state of the whole insulating paper. However, it is unable to reveal the aging state of insulating paper in specific regions.

3.3. Chemical Indicator Testing

During the aging process of oil–paper insulation, there are complex chemical reactions existing in oil–paper insulation. Thus, there are various small molecule compounds (such as furfural, methanol, ethanol, formic acid, and acetic acid) produced with the above chemical reactions and dissolved in the insulating oil. In the literature [35], the quantitative relationship between the above chemical indicators and the insulating paper’s DP has been proposed. Thus, the aging degree of the insulating paper can be researched by detecting the concentration of the above chemical indicators in the insulating oil. A schematic diagram of the dissolved chemical indicators analysis is shown in Figure 7.

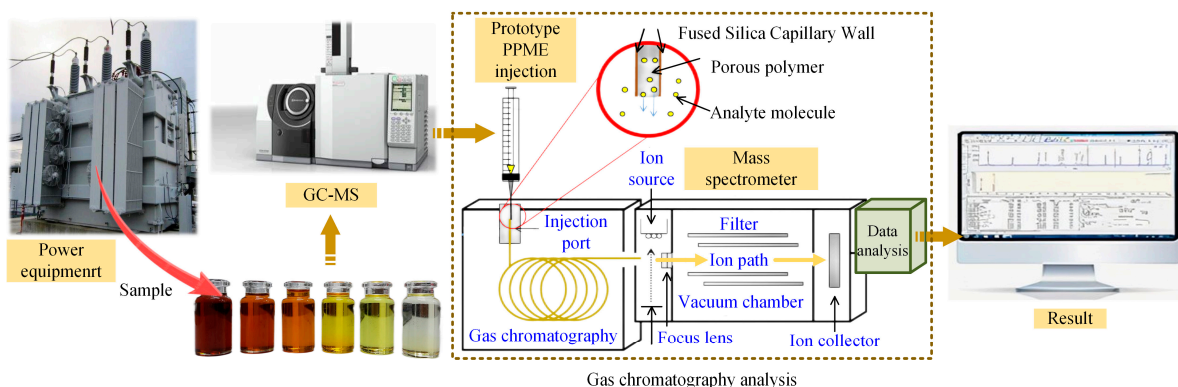


Figure 7. A schematic diagram of dissolved chemical indicators analysis.

3.3.1. Furfural

Furan compounds (such as furfural) are only produced with insulating paper's aging. The oxidative cracking of the insulating oil does not produce furan compounds [36]. Therefore, furan compounds are the ideal chemical indicator for researching the aging state of insulating paper. Furfural has strong thermal stability, of which pyrolysis is not easy under high temperatures. Thus, the content of furfural dissolved in the insulating oil is higher than other furan compounds, which means that furfural is a better chemical indicator than other furan compounds for researching the aging state of the insulating paper. The existing research proves that there is a semi-logarithmic linear relationship between the content of furfural and the DP of the insulating paper, as shown in Table 2 (Chengdong equation, Burton equation, and Vuarchex equation) [37–39].

Table 2. Equations for the content of furfural and DP of the insulating paper.

Number	Equation Name	The Expression of Equation
1	Chengdong	$\lg(C_{fur}) = 1.5 - 0.0035 * DP$
2	Burton	$\lg(C_{fur}) = 2.5 - 0.005 * DP$
3	Vuarchex	$\lg(C_{fur}) = 2.6 - 0.0049 * DP$

Where C_{fur} is the content of furfural dissolved in the insulating oil. According to <DL/T596-1996 Preventive Test for Electric Power Equipment> [40], while the furfural content exceeds 4 mg/L, the oil–paper insulation is at a serious degree of aging and its operating life is near the end.

However, there are still some failings with the above evaluation method: (1) some of the furfural is lost during the operation of pressure oil filtration and high vacuum oil filtration, which causes a deviation in the evaluation results, (2) the generation rate of furfural in the early aging stage is extremely low [41]; thus, the furfural content is not reliable as a chemical indicator to evaluate the aging state of insulating paper in the early aging stage, and (3) the furfural content cannot reveal the aging state of the insulating paper in specific regions.

3.3.2. Methanol and Ethanol

During the aging process of insulating paper, there are alcohol compounds produced and dissolved in the insulating oil, such as methanol and ethanol. The detection techniques for the methanol and ethanol content dissolved in the insulating oil mainly include gas chromatography and Raman spectroscopy. J. Jalbert et al. [42] and Wang Dongdong et al. [43] have proved that methanol and ethanol have two main advantages compared to other chemical indicators: strong stability and high content. According to the existing research [44], there is a linear quantitative relationship between the methanol content and the number of 1,4- β glycosidic bonds broken in the cellulose chains during the insulating paper's aging process. Therefore, the methanol content can be an effective chemical indicator for evaluating the aging degree of the insulating paper. Peng Lei has adopted spectroscopic techniques to detect the methanol content dissolved in the insulating oil, and a quantitative relationship between the methanol content and the degree of polymerization (DP) of the insulating paper has been proposed [25], as shown in Equation (1).

$$DP = 781.56 - 1.60 * C_{met} \quad (1)$$

where C_{met} represents the methanol content dissolved in the insulating oil. In addition, Schaut et al. [45] have proved that the methanol content is exponentially correlated with the furfural content dissolved in the insulating oil. Laurichesse et al. [46] have proposed that methanol is mainly produced in the early aging stage of insulating paper ($DP > 900$). Thus, methanol is a better chemical indicator for researching the early aging stage of insulating paper compared with furfural. Zhang et al. have researched the relationship between the ethanol content dissolved in the insulating oil and the DP of the insulating paper. Further,

a lifespan model has been proposed based on the above relationship [47]. In reference [48], the chemical reactions between the ethanol and acid compounds have been researched, and the reduction mechanism of the ethanol content caused by the acid compounds has been analyzed. However, due to the operation of pressure oil filtration and high vacuum oil filtration, some of the methanol and ethanol dissolved in the insulating oil is lost, which causes a deviation in the evaluation results [49]. Meanwhile, the methanol and ethanol contents dissolved in the insulating oil are only effective for evaluating the average aging degree of the insulating paper and are unable to uncover the aging state of the insulating paper in specific regions.

3.3.3. Formic Acid and Acetic Acid

L. Lundgaard et al. have proved that there are small molecular organic acids (such as formic acid and acetic acid) produced during the aging process of insulating paper and dissolved in the insulating oil [50]. Meanwhile, there are big molecular organic acids (such as stearic acid and naphthenic acid) produced during the aging process of insulating oil. Yang et al. have proved that formic acid and acetic acid can significantly accelerate the aging of insulating paper, which means that small molecular organic acids have a strong correlation with the aging of insulating paper [51]. Li Qingmin et al. have developed a standard detection method for the organic acid content dissolved in insulating oil, which provides technical support for establishing the quantitative relationship between small molecular organic acids content dissolved in the insulating oil and the degree of polymerization (DP) of the insulating paper [52]. In summary, small molecular organic acids (such as formic acid and acetic acid) are potential chemical indicators for evaluating the aging state of insulating paper.

However, Wang Dongdong et al. have proved that there are esterification reactions between small molecular alcohols and organic acids that happen during the middle and late aging stages of oil–paper insulation, resulting in the organic acid content dissolved in the insulating oil decreasing [53]. The types of organic acids which dominate the above esterification reactions are not clear. Considering that the loss of organic acids can cause the evaluation results of the insulating paper’s aging degree to be unreliable, it is necessary and important to clarify the mechanism of the above esterification reactions and improve the evaluation theory for the insulating paper’s aging state based on formic acid and acetic acid.

3.4. The Aging Kinetic Model

The evaluation methods for the insulating paper’s aging degree introduced in Sections 3.1–3.3 are based on experimental testing. In contrast, the aging kinetic model is an evaluation method based on theoretical calculation and law analysis. Aging kinetic models are adopted to describe the decline process of the insulating paper’s DP. Further, a quantitative analysis of the aging degree of insulation paper is carried out based on aging kinetic models. According to the existing research [54–56], common aging kinetic models mainly include the first-order aging kinetic model, the second-order aging kinetic model, and the cumulative loss of the degree of polymerization kinetic model. The development process of the above aging kinetic models is shown in Figure 8.

The cellulose chain in insulating paper is a linear polymer, which is composed of glucose monomers linked with each other. Based on the linear polymer degradation kinetics model and the first-order random chain scission hypothesis, Ekenstam established the quantitative relationship between the reciprocal of the insulating paper’s DP and the aging time (i.e., the first-order aging kinetic model, as shown in Equation (2) [54].

$$\frac{1}{DP_t} - \frac{1}{DP_0} = k * t \quad (2)$$

where k is the aging rate constant of insulating paper, t is the aging time, DP_0 is the initial DP of the unaged insulating paper, and DP_t is the DP of the insulating paper after aging time t .

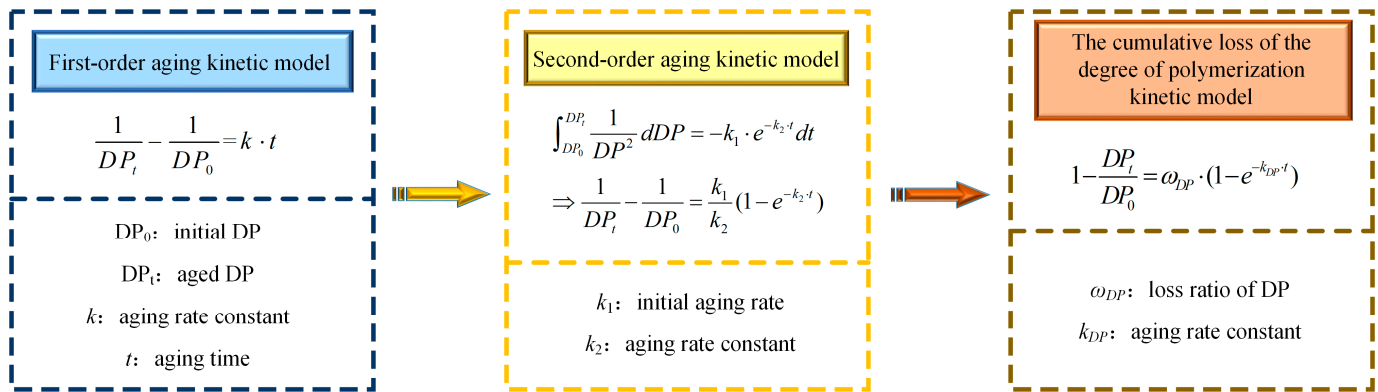


Figure 8. The development process of these aging kinetic models.

However, Heywood has proposed that while the insulating paper's DP drops to a certain value, the quantitative relationship between the DP and the aging time of the insulating paper gradually deviates from the first-order kinetic model [57]. In this case, the aging rate k is no longer constant, which is defined as the LODP phenomenon (leveling-off degree of polymerization). In other words, the k shown in Equation (2) should change with the aging time, as shown in Equation (3).

$$k(t) = \lim_{\Delta t \rightarrow 0} \frac{m_t}{N * \Delta t} = k_1 * e^{-k_2 * t} \quad (3)$$

where k_1 and k_2 are constants related to the initial moisture content of the insulating paper. Then, based on a series of theoretical calculations, the quantitative relationship between the aging time t , the aging rate $k(t)$, and the insulating paper's DP is shown in Equation (4) (i.e., the second-order aging kinetic model, as shown in Equation (4) [55].

$$\int_{DP_0}^{DP_t} \frac{1}{DP^2} dDP = -k_1 * e^{-k_2 * t} dt \Rightarrow \frac{1}{DP_t} - \frac{1}{DP_0} = \frac{k_1}{k_2} (1 - e^{-k_2 * t}) \quad (4)$$

It has been widely recognized that the second-order aging kinetic model can accurately reflect the change law of DP during the insulating paper's aging process. However, there is no practical physical meaning for the aging constants k_1 and k_2 in Equation (3). Based on the theoretical analysis of the cellulose chain's break, Ding et al. have established the "DP loss percentage" aging kinetic model [58], as shown in Equation (5).

$$\omega(t) = 1 - \frac{DP_t}{DP_0} = \omega_{DP} (1 - e^{-k_{DP} * t}) \quad (5)$$

where ω_{DP} is the amplitude of the attenuation function. k_{DP} is the break rate of the cellulose chain, which is related to the concentration of the aging by-products in the insulating paper. $\omega(t)$ represents the "DP loss" capacity. $\omega(t)$ can be adapted to reflect the deterioration degree of the insulating paper, as shown in Equation (6).

$$\omega(t) = \begin{cases} 0 & \text{Polymer material has not fully degraded} \\ 1 & \text{Polymer material has not degraded} \end{cases} \quad (6)$$

However, the above equation is only effective for researching the insulating paper's aging under the reference temperature, which cannot be directly applied to the insulating paper's aging under the dynamic temperature field. Based on the time–temperature superposition theory [59], the increase in aging temperature and the extension of aging time have the same effect on the aging process of the insulating paper. This time–temperature property can be expressed as Equation (7).

$$t_{ref} * T_{ref} = t * T \quad (7)$$

where T_{ref} is the reference aging temperature, and t_{ref} is the required aging time to reach the given aging degree at T_{ref} . Based on the Arrhenius theory [60], the aging rate k_i at different aging temperatures can be expressed as Equation (8).

$$k_i = A * e^{-\frac{E_a}{R * T_i}} \quad (8)$$

where A is the pre-exponential factor related to the moisture content of the insulating paper. R is the gas constant (8.314 J/mol K). E_a is the activation energy (103 kJ/mol). The ratio (α_T) of the aging rate at reference temperature T_{ref} to the aging rate at practical temperature T is shown in Equation (9).

$$\alpha_T = \frac{T}{T_{ref}} = \frac{k}{k_{ref}} = e^{\frac{E_a}{R} (\frac{1}{T_{ref}} - \frac{1}{T})} \quad (9)$$

Based on the above discussion, the aging kinetic model shown in Equation (5) can be improved in Equation (10) (i.e., the cumulative loss of the degree of polymerization kinetic model), which can reflect the insulating paper's aging process at different aging temperatures [56].

$$1 - \frac{DP_t}{DP_0} = \omega_{DP} * (1 - e^{-k_{DP} * t_{ref}}) s.t. \left\{ \begin{array}{l} t_{ref} = t * \exp[E_a(1/T_{ref} - 1/T)/R] \\ k_{DP} \propto F(mc\%) \\ \omega_{DP} \propto G(mc\%) \end{array} \right. \quad (10)$$

In summary, while the aging temperature, the aging time, and the moisture content have been defined, the aging kinetic models can be adopted to predict the change law of the insulating paper's DP. The aging kinetic models have the advantages of low dependence on model parameters and a simple calculation process. Thus, they have been widely adopted for evaluating the insulating paper's aging degree under laboratory conditions.

However, there are some limitations to the aging kinetic models. The aging kinetic models are suitable for researching the aging process of a single polymer material and a certain chemical reaction. However, there are lots of polymer materials existing in the insulation system, and various chemical reactions are carried out simultaneously. Therefore, the aging process in oil–paper insulation is too complex for the aging kinetic models. In addition, during the operation of the power equipment, the moisture content and aging temperature in the oil–paper insulation are dynamic. Therefore, it is not reasonable to adopt a constant to define the moisture content and aging temperature in the aging kinetic models. In conclusion, the aging kinetic models are only effective for evaluating the insulating paper's aging degree under ideal laboratory conditions.

3.5. The Optical Diffraction Spectra and Imaging Technique

During the aging process of oil–paper insulation, the morphology and properties of the oil–paper insulation change constantly. Thus, the interaction between the oil–paper insulation and light changes constantly during the aging process, which means that optical technology has full potential for evaluating the aging degree of oil–paper insulation. To research the change laws of the oil–paper insulation's microstructure during the aging process and obtain the microscopic characteristics of various molecules, lots of optical imaging methods based on X-ray photoelectron spectroscopic (XPS) and optical coherence tomography (OCT) have been reported [61,62]. A schematic diagram of the X-ray diffraction spectrum technique is shown in Figure 9 as an example.

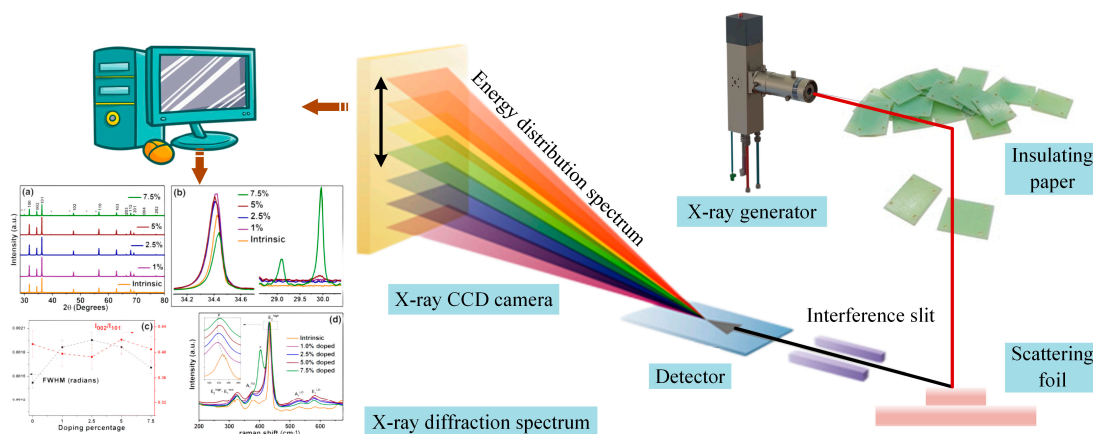


Figure 9. A schematic diagram of the X-ray diffraction spectrum technique.

The microstructure of insulating paper mainly includes the superposition of molecular chains, amorphous structure, and crystalline structure. Due to the wavelength of X-rays (0.05–0.25 nm) and the distance between the cellulose molecules being roughly the same, the XPS technique has been adopted to research the change laws of the insulating paper's microstructure during the aging process. Liao et al. proposed the change laws of the aging by-products under different aging temperatures and different oil–paper ratios and qualitatively analyzed the change laws of the insulating paper's microstructure during the aging process [63]. Based on the XPS technique, Yang et al. have researched the influence mechanism of the aging effect on the insulating paper's microstructure and further analyzed the decreasing process of the insulating paper's DP based on the change laws of the insulating paper's microstructure [61].

Although the XPS technique can effectively analyze the microscopic mechanism in aging oil–paper insulation, it is unable to evaluate the aging degree of the oil–paper insulation. In contrast, optical coherence imaging based on fiber imaging technology (OCT) can achieve this goal [62]. In reference [64], the aging characteristic information has been extracted from the sub-surface structure images of insulating paper based on microscopic imaging technology. Then, supervised learning has been adopted to complete the condition assessment. However, this technique is unable to research the microscopic reaction mechanism during the aging process, so optical coherence imaging (OCT) based on fiber imaging technology has been proposed. Further, the statistical algorithm has been adopted to evaluate the service life of oil–paper insulation.

In summary, XPS and OCT technologies based on optical imaging techniques are effective for analyzing the microscopic mechanism of various molecules during oil–paper insulation's aging process. However, there are some limitations with the two techniques, such as the fact that the sampling and imaging of insulating paper are both difficult. The condition assessment process based on the OCT technique can be achieved by (1) using handheld OCT systems to obtain OCT images of oil–paper insulation's different regions during normal maintenance, and (2) using different optical fiber OCT probes connected to a single OCT system [65]. Therefore, for collecting the OCT data, the power equipment is required to be under a maintenance hood or pre-installed with optical fiber probes, which are difficult conditions to meet for most in-service power equipment.

4. Techniques for Evaluating the Moisture Content of Oil–Paper Insulation

4.1. Karl Fischer Titration Technique

The Karl Fischer titration technique is an electrochemical analysis technique for testing the moisture content of the oil–paper insulation samples, which is proposed by Karl Fischer [66]. The Karl Fischer titration technique can be divided into the Karl Fischer volumetric technique and the Karl Fischer coulomb technique. As for the Karl Fischer volumetric technique, the volume of the added reagent can be measured, and further, the

moisture content of the oil–paper insulation system can be calculated by a stoichiometric equation. However, the sensitivity of volumetric titration is limited to about 10 μg [67]. Considering that the moisture content of the oil–paper insulation is very low, the Karl Fischer volumetric technique is hardly applicable for evaluating the moisture content of oil–paper insulation. In contrast, the sensitivity of the coulomb technique can reach down to 1 ppm (0.0001%). Thus, the Karl Fischer coulomb technique can be adopted to evaluate the moisture content of oil–paper insulation in the power equipment.

The principle of the Karl Fischer coulomb technique is as follows: While the Karl Fischer reagent in the electrolytic cell reaches equilibrium, the researcher adds the testing samples (the insulating paper or insulating oil) into the electrolytic cell. Then, the water molecule in the testing samples can participate in the redox reaction between iodine and sulfur dioxide. During the above redox reaction, the iodine on the cathode undergoes the oxidation reaction, and the iodine on the anode undergoes the reduction reaction. Thus, the iodine consumed on the cathode can be regenerated on the anode of the electrolytic cell. The iodine generated on the anode can consume the water molecules existing in the testing samples, continuously. The equations for the above chemical reactions are shown in Equations (11) and (12) [68].



According to the above chemical reaction equations, 1 mole of the water molecule is required for the oxidation reaction between 1 mole of the iodine and 1 mole of the sulfur dioxide. Therefore, during the testing process, the total electricity for electrolyzing all iodine is equivalent to the total electricity for electrolyzing all water molecules in the testing samples. Further, the moisture content of the testing samples can be calculated by Equation (13), where Q is the consumed total electricity (mC) during the testing process, and W is the moisture content (μg) of the testing samples.

$$W = 0.0933 \cdot Q \quad (13)$$

In summary, the Karl Fischer titration technique can directly and accurately obtain the moisture content of the insulating paper and insulating oil. However, there are some limitations to the Karl Fischer titration technique applied in field testing: (1) It belongs to the offline testing technique, and this technique requires researchers to take the oil–paper insulation samples from power equipment. Thus, the sampling operation can cause destructive damage to the oil–paper insulation of in-service power equipment. (2) During the sampling process, the power equipment needs to be powered off and its insulating paper needs to be taken out. This operation can cause its oil–paper insulation system to be exposed to the field environment, and the impurities (such as water molecules and oxygen) in the air can invade the oil–paper insulation. Further, the evaluation result of the oil–paper insulation’s moisture content is not accurate and reliable. Meanwhile, the above impurities can accelerate the degradation rate of the oil–paper insulation. According to the above discussion, the Karl Fischer titration technique is not suitable for evaluating the moisture content of oil–paper insulation in in-service power equipment. It can be adopted to evaluate the moisture content of the oil–paper insulation under laboratory conditions.

4.2. Cellulose–Water Adsorption Isotherm

In operating power equipment, the water molecules in the insulating paper diffuses into the insulating oil under the influence of oil flowing and temperature field. The above diffusion process can cause the moisture content of the insulating paper to decrease. Meanwhile, due to the strong adsorption capacity of the insulating paper to the water molecules, some water molecules dissolved in the insulating oil can accumulate in the insulating paper. The above accumulation process can cause the insulating paper’s moisture

content to increase. While the accumulation rate of the water molecules in the insulating paper is equivalent to the diffusion rate of that, the process of the water molecules moving between the insulating paper and the insulating oil reaches the dynamic equilibrium, which is defined as the cellulose–water adsorption isotherm [69].

Langmuir et al. first proposed the concept of cellulose–water adsorption isotherms in 1916 and pointed out that the moisture content of the insulating paper can be evaluated by the moisture content of the insulating oil and the water vapor pressure on the insulating paper’s surface [70]. However, the Langmuir cellulose–water adsorption isotherm is only suitable for evaluating insulating paper with low moisture content, which is not effective for evaluating severely damp oil–paper insulation. Meanwhile, the above cellulose–water adsorption isotherm model does not take into account the interaction between water molecules. Therefore, based on the moisture content of the insulating oil and the water vapor pressure on the insulating paper’s surface, Fessler and Rouse proposed the Freundlich adsorption isotherm model to evaluate the moisture content of the insulating paper at a specific temperature, as shown in Equation (14) [71].

$$WCP = 2.173 * 10^{-7} * P_v^{0.6685} * e^{\frac{4725.6}{T+273}} \quad (14)$$

where T is the operating temperature of the oil–paper insulation. WCP is the moisture content of the insulating paper. P_v is the water vapor pressure on the insulating paper’s surface.

In addition, Mateusz and Piotr have studied the cellulose–water adsorption isotherm model of oil–paper insulations, which are composed of different types of insulating oil (mineral oil, natural ester, and synthetic ester) and cellulose insulating paper [72]. Meanwhile, the reliability of the above cellulose–water adsorption isotherm model has been verified based on a comparison of 12 types of oil–paper insulations, whose insulating paper has different aging degrees and moisture contents under laboratory conditions.

However, Equation (14) is based on the equilibrium between the operating temperature and the water vapor pressure. With the operating temperature changing dynamically, the water molecules will enter or leave the insulating paper until the new moisture distribution equilibrium is established. Thus, Guidi et al. have researched the time constant of the water molecules moving between the insulating paper and the insulating oil based on the insulation geometry and diffusion coefficient, as shown in Equation (15) [73].

$$\begin{cases} \tau = \frac{4d^2}{\pi^2 D_p} \\ D_p = D_0 e^{k * WCP + E_a(\frac{1}{T_0} - \frac{1}{T})} \end{cases} \quad (15)$$

where τ is the time constant. d is the thickness of the insulating paper. T is the Kelvin temperature constant. D_p is a constant. D_0 is the diffusion coefficient under the temperature T_0 (298K). E_a is the activation energy of the moisture diffusion.

The Freundlich isotherm is based on the assumption of thermodynamic equilibrium. However, the temperature field in power equipment always cycles for 24 h, and the diffusion time constant is always much longer than 24 h. Therefore, in operating power equipment, the moisture distribution between the insulating paper and the insulating oil cannot reach the actual equilibrium. As a result, due to the water molecule diffuses lagging behind the temperature field changes, the calculation of WCP is very complicated with Equation (14).

4.3. Oil–Paper Moisture Balance Curve Technique

Due to the hydrophilicity of insulating paper and the hydrophobicity of insulating oil, 99% of the water molecules in the oil–paper insulation system are distributed in the insulating paper. Under the influence of the oil flowing and the temperature field, the water molecules move between the insulating paper and the insulating oil. Finally, the above moisture diffusion process maintains a dynamic equilibrium. In summary, the moisture

content of the insulating paper can be calculated by the moisture content of the insulating oil, as shown in Figure 10 [74].



Figure 10. A schematic diagram of the oil–paper moisture balance curve technique.

As shown in Equation (14), the water vapor pressure on the insulating paper’s surface P_v is the core parameter for calculating the moisture content of the insulating paper. Thus, Equation (16) has been proposed for calculating the P_v based on the moisture activity in the insulating oil [75].

$$a_w = \frac{P_v(T)}{P_0(T)} = \frac{WCO}{S(T)} \quad (16)$$

where T is the operating temperature of the oil–paper insulation. $S(T)$ is the solubility of water molecules dissolved in the insulating oil at T . WCO is the moisture content of the insulating oil. $P_0(T)$ is the pure water vapor pressure at T , which can be calculated by Equation (17).

$$P_0(T) = 0.00603 * e^{\frac{17,502 * T}{240,94 + T}} \quad (17)$$

Considering that the water vapor pressure above the dilute solution changes linearly with the concentration of the dilute solution, $P_v(T)$ can also be calculated by the solubility of water molecules dissolved in the insulating oil $S(T)$ and the moisture content of the insulating oil, as shown in Equation (18).

$$S(T) = 10^{A - \frac{B}{273 + T}} \quad (18)$$

where A and B are the coefficients of solubility. Based on Equation (18), Oommen et al. have researched the curves of moisture content of the insulating oil and insulating paper with experiments. Then, the oil–paper moisture balance curve has been obtained by studying the change laws of the above curves [76]. Zhou Lijun et al. have researched the influence of the operating temperature on the water diffusion process and constructed a quantitative relationship between the temperature, the moisture content of the insulating oil, and the moisture content of the insulating paper. Further, the oil–paper moisture balance curve at each temperature has been obtained [77]. In summary, the moisture content of the insulating oil and oil–paper moisture balance curve can be adopted to analyze the moisture content of the insulating paper. The only required sample is the insulating oil, which means there is no destructive damage to the insulating paper. However, there are excessive idealized assumptions existing in the oil–paper moisture balance curve, and the calculation error of the moisture content of the insulating paper can even reach 200%.

4.4. Measurement with Moisture Sensors

Compared with moisture active probes, optical fiber-based moisture sensors have better geometry structures and electrical characteristics, which can accurately detect the moisture content of power equipment’s oil–paper insulation without being affected by the electromagnetic field in the high-voltage conditions and temperature fields in high-

temperature conditions [78]. The principle for monitoring oil–paper insulation’s moisture content by optical fiber-based moisture sensors is shown in Figure 11. Based on the miniature and flexible structure, optical fiber-based moisture sensors can be easily embedded in the winding structure. Thus, optical fiber-based moisture sensors are considered the ideal sensors for almost any location in power equipment. Further, optical fiber-based moisture sensors can be multiplexed along the path of a single fiber optic cable, which can be adopted to evaluate the moisture gradient across the entire power equipment.

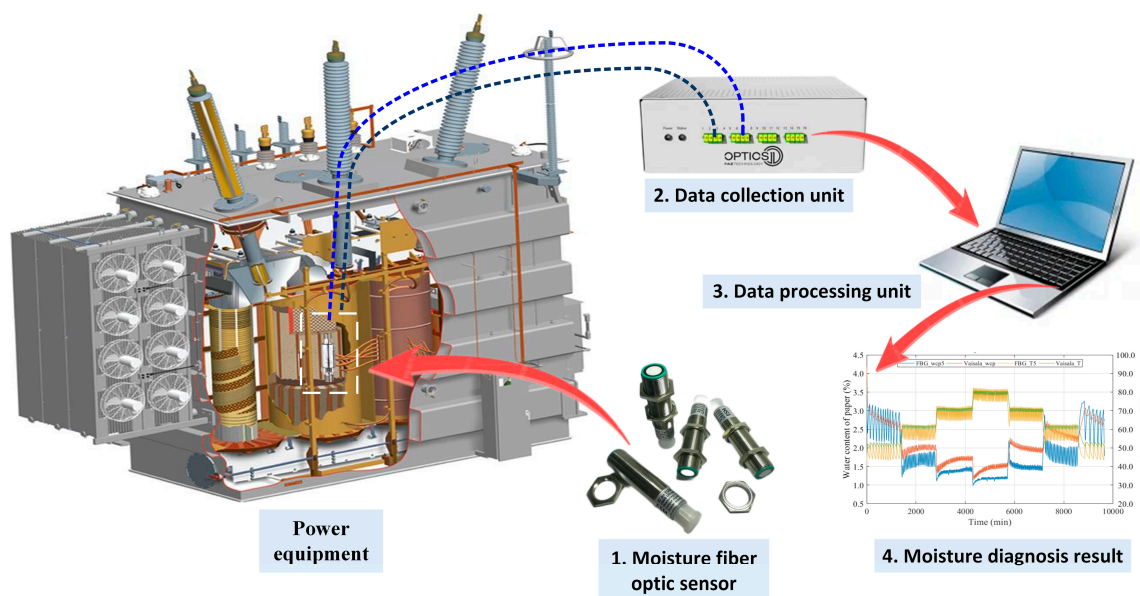


Figure 11. A schematic diagram of measurements by optical fiber-based moisture sensors.

In reference [79], optical fiber-based moisture sensors have been adopted to achieve the online monitoring of oil–paper insulation’s moisture content under the step cycle heat load. The research results show that optical fiber-based moisture sensors have excellent performance under different working conditions and harsh electromagnetic environments. Their miniature size and multiplexing characteristic can be adopted to analyze the moisture distribution in power equipment. During continuous online monitoring, optical fiber-based moisture sensors can provide early warnings for power equipment’s abnormal phenomena.

Compared with the cellulose–water adsorption isotherm technique, the optical fiber-based moisture sensors can realize the online monitoring of the insulating paper’s moisture content without measuring the insulating oil’s moisture content. This characteristic can effectively reduce the error of the evaluation results, which is caused by the loss of the insulating oil’s moisture content during the oil filtering and oil changing. In addition, compared with the traditional moisture analysis technique, the optical fiber-based moisture sensors are more flexible, which can monitor in real-time the moisture content of the insulating paper at the power equipment’s different regions. However, the sensors can affect the electric field distribution in the oil–paper insulation system. Meanwhile, the impurities dissolved in the insulating oil can accumulate near the installation position of the sensors, resulting in the reduction of the breakdown voltage and electrical performance of the oil–paper insulation. Moreover, the sensors are subjected to the synergistic influence of high temperature, discharge, vibration, and other factors in the operating power equipment. The synergistic influence can damage the sensors and decrease their monitoring accuracy. Therefore, lots of money is required for the repair and maintenance of optical fiber-based moisture sensors.

5. A Comprehensive Evaluation Technique: Dielectric Response Technique

5.1. Introduction of the Dielectric Response Technique

According to the introduction in Sections 3 and 4, the traditional evaluation techniques can only evaluate the single insulation state (aging degree or moisture content) of oil–paper insulation and cannot simultaneously evaluate the aging degree and moisture content alone. In contrast [80], dielectric response techniques can be adopted to evaluate oil–paper insulation’s aging degree and moisture content simultaneously, which have been proposed based on the dielectric physics theory. Specifically, the dielectric response data can reflect various dielectric response behaviors of various polar molecules existing in the oil–paper insulation system under various electric field excitations. The aging degree and moisture content of the oil–paper insulation can change the number and concentration of the above polar molecules and further change the dielectric response data of oil–paper insulation. Thus, there is rich feature information about oil–paper insulation’s aging degree and moisture content existing in its dielectric response data. In summary, the dielectric response techniques can be adapted to not only research the microscopic dielectric response behavior of the polar molecules existing in oil–paper insulation but also evaluate the aging degree and moisture content of oil–paper insulation.

Based on the different types of electric field excitations applied to oil–paper insulation, the dielectric response techniques can be divided into the time-domain dielectric response technique and the frequency-domain dielectric response technique. The time-domain dielectric response technique can be divided into the recovery voltage method (RVM) and the polarization and depolarization current method (PDC). Meanwhile, the frequency domain dielectric response technique is only the frequency domain spectrum (FDS). The technical details and research results of the above dielectric response techniques are as follows:

5.1.1. Recovery Voltage Method (RVM)

The recovery voltage method (RVM) is a non-destructive testing technique for evaluating oil–paper insulation’s aging degree and moisture content by researching the recovery voltage curve after the polarization and depolarization process of the oil–paper insulation. The testing principle and typical testing curves of RVM are shown in Figure 12 [81]. In Figure 12, while switch S_1 is turned off, the DC voltage source U_0 charges the oil–paper insulation. With the continuous charging by U_0 , the voltage on the oil–paper insulation gradually increases. While the voltage reaches the maximum value, switch S_1 is opened, and switch S_2 is closed. Further, the oil–paper insulation loses the excitation of the DC voltage source U_0 and enters the discharge process. The voltage on the oil–paper insulation gradually decays to 0, and then the measurement of the recovery voltage curve is completed.

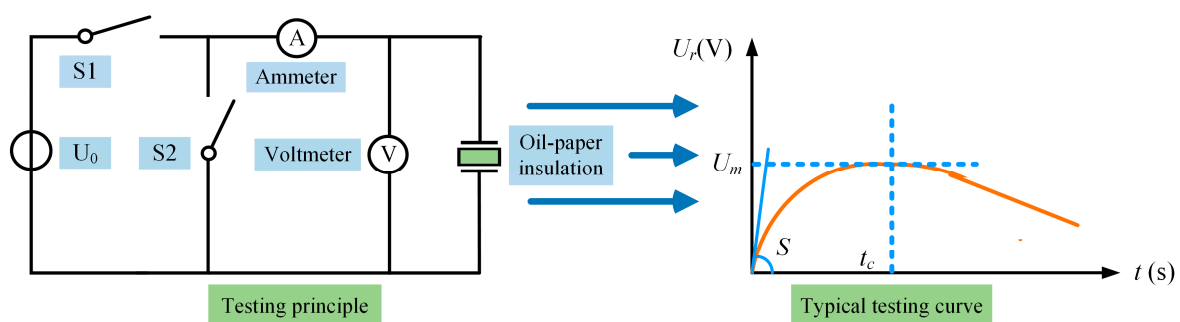


Figure 12. The testing principle and typical testing curves of the recovery voltage method.

The existing research has shown that there is a strong correlation between the aging degree and moisture content of the oil–paper insulation and the maximum value of the recovery voltage curve, the central time constant, and the initial slope of the RVM curve [82–84]. Based on the RVM curve of the oil–paper insulation with different aging degrees, Zhou Lijun et al. [20]

have obtained the following conclusions: (1) The maximum value of the recovery voltage curve increases with the increase in the charging voltage and is significantly affected by the charging time. (2) The central time constant is not easily changed by the external testing conditions (3) The initial slope of the RVM curve is positively correlated with the ratio between the charging time and discharging time, and it is less affected by the charging voltage. However, the above feature parameters are extracted based on the shape of the RVM curve, which has no practical physical meaning. In contrast, the feature parameters in the dielectric response models have a clear physical meaning, which can reflect the dielectric response characteristic of polar molecules. In reference [85], it has been proved that the extended Debye model is effective for reflecting the time-domain dielectric response of the oil–paper insulation. Yang et al. have proposed that the branch resistance, branch capacitance, and branch time constant in the extended Debye model can reflect the aging degree of the oil–paper insulation system [86]. Then, based on the feature parameters, Sarkar et al. established a standard dielectric response eigenvector group to reflect the oil–paper insulation’s aging degree. Meanwhile, the multivariate features expert system has been adapted to evaluate the aging degree of the insulating paper [87]. The above research studies have proved the effectiveness of RVM in evaluating the aging degree and moisture content of oil–paper insulation.

5.1.2. Polarization and Depolarization Current (PDC) Technique

The PDC technique is a non-destructive testing technique for evaluating the aging degree and moisture content of oil–paper insulation based on researching the polarization and depolarization currents through the oil–paper insulation system. One research study [88] has proved that the PDC technique can distinguish the insulation information of the insulating paper and insulating oil. The testing principle and typical testing curves of the PDC technique are shown in Figure 13. Similar to the measurement process of RVM, the PDC measurement is also carried out under the excitation of the DC voltage source. The whole process can also be divided into the charging stage and discharging stage. When switch S is turned to the left, the charging circuit is connected. The DC voltage source U_0 charges the oil–paper insulation to generate the polarization current i_p , and the polarization current curve follows the law of exponential decay. If the charging time is long enough, the attenuation of the polarization current will gradually tend to be stable (not 0). While the charging time reaches the preset value t_p , the switch S is closed and the discharging circuit is connected. The oil–paper insulation is reversely discharged to generate the depolarization current i_d , which has a similar decay law to the polarization current. However, compared to the polarization current, the depolarization current will gradually decay to 0 as the discharging time increases.

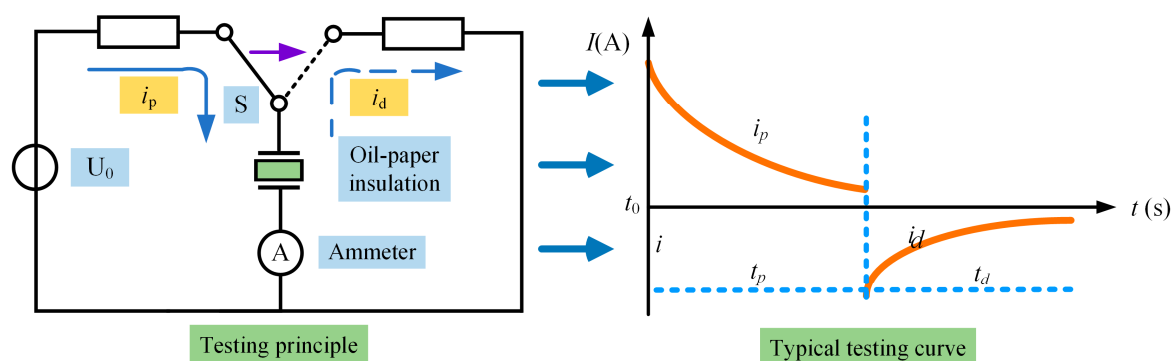


Figure 13. The testing principle and typical testing curves of the PDC technique.

Saha et al. have researched the main factors which can affect the PDC testing curve, such as the excitation voltage, insulation geometry, testing time, and testing temperature [89]. In reference [90], the polarization electric quantity has been calculated based on the integral operation and the testing polarization current, and the correlation between its slope and the oil–paper insulation’s moisture content has been proved. In reference [91], the feature parameters have been extracted based on the terminal two-point analysis method and the PDC data, which can reflect the insulation state of the oil–paper insulation. Considering that the extended Debye model is effective for researching the time-domain dielectric response information of oil–paper insulation, Saha et al. have identified the resistor and capacitor in the extended Debye model and extracted the feature parameters (the amplitude and corresponding sub-relaxation time constant in each branch) from PDC data. Then, the correlation between the insulation state of the oil–paper insulation and the above model parameters has been established [92]. Further, Saha et al. have pointed out that the branch model parameters corresponding to the largest time constant mainly reflect the insulating paper’s insulation state, and the branch model parameters corresponding to the small time constant mainly reflect the insulating oil’s insulation state [93]. In addition, the choice of the largest time constant branch in the extended Debye model is often determined based on the fitting analysis, which lacks clear criteria. Given this issue, Cai et al. proposed the extended Debye model parameters identification technique based on the depolarization current differential line [94]. In reference [95], various feature parameters have been extracted from PDC data and the aging degree and moisture content of oil–paper insulation have been evaluated based on the above feature parameters and an expert system.

5.1.3. Frequency Domain Spectrum (FDS)

The frequency domain spectrum (FDS) of the oil–paper insulation system represents its frequency dielectric response information under the alternating electric field [96]. The oil–paper insulation’s FDS data include the complex relative permittivity $\varepsilon^*(\omega)$, complex capacitance $C^*(\omega)$, dielectric loss factor $\tan \delta$, and complex polarizability $\chi^*(\omega)$. The correlation between the above FDS data is shown in Equation (19).

$$\begin{cases} \frac{C^*(\omega)}{C_0} = \varepsilon^*(\omega) = \chi^*(\omega) + \varepsilon_\infty \\ \frac{\varepsilon''(\omega)}{\varepsilon'(\omega)} = \tan \delta \end{cases} \quad (19)$$

where C_0 is the geometric capacitance of the oil–paper insulation system. ε_∞ is the optical frequency dielectric constant. In addition, the FDS data (except $\tan \delta$) are in the form of complex numbers. Specifically, the real part of the FDS data can reflect the energy storage part of the oil–paper insulation, which can be simulated by the capacitance in the equivalent circuit model. The real part data mainly represent the polarization strength characteristics of the oil–paper insulation. The imaginary part of the FDS data can reflect the energy loss part of the oil–paper insulation, which can be simulated by the resistance in the equivalent circuit model. The imaginary part data mainly represent the polarization loss characteristics of the oil–paper insulation. The dielectric loss factor $\tan \delta$ is the ratio between the imaginary part to the real part of the complex relative permittivity $\varepsilon^*(\omega)$.

The FDS data can be obtained by applying the AC excitation on the oil–paper insulation, and the FDS data are tested point-by-point from high frequency to low frequency. The core elements in the measurement circuit include the sinusoidal alternating voltage source, voltmeter, and ammeter. The testing principle and typical testing curves of the FDS technique are shown in Figure 14.

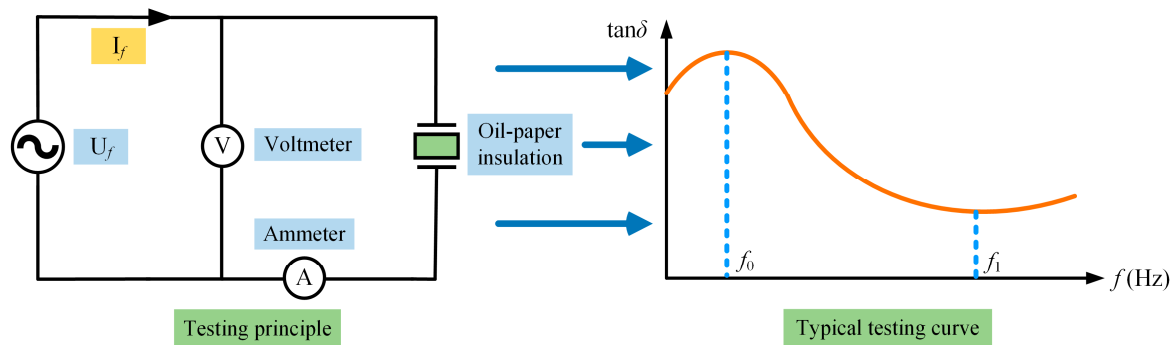


Figure 14. The testing principle and typical testing curves of the FDS technique.

For the frequency domain dielectric response of oil–paper insulation, the polarization processes of different polar molecules have been established at different frequencies. With the frequency of the excitation field increasing, more and more polarization processes cannot be established in the high frequency. This phenomenon causes the oil–paper insulation’s polarization intensity to decrease and the FDS curve to decrease in high frequency. It is defined as the ‘frequency dependence’. In reference [97], it has been proved that the insulating paper’s aging information is contained in the FDS data at the low-frequency region, and the dominant factor of the FDS data at the low-frequency region is the conductance effect. Therefore, Fan et al. have extracted the feature parameters from the FDS data at the low-frequency region and established the quantitative relationship between these feature parameters and the insulating paper’s aging degree [98]. It has been proved that the FDS data at the high-frequency region are dominated by the oil–paper insulation’s moisture content. Further, Fan et al. have obtained the feature parameters from the FDS data at the high-frequency region, which can reflect the oil–paper insulation’s moisture content [99], as shown in Equation (20). In summary, the FDS data are effective for evaluating the oil–paper insulation’s aging degree and moisture content.

$$\begin{cases} mc\% = 7.028 - 8.885 \cdot \text{EXP}(-IV/33.791) \\ mc\% = 12.906 + 1.862 \cdot \ln(\tan \delta_{\min}) \\ mc\% = 3.869 - 3.316 \cdot \text{EXP}(-f_{\min}/870.115) \end{cases} \quad (20)$$

In the above equations, IV represents the integral value of measured dispersion loss for the sample. $\tan \delta_{\min}$ and f_{\min} represent the minimum value of the dispersion loss of the sample and its corresponding frequency, respectively. It can be found from the above equations that the dispersion loss value increases regularly with the moisture content in the sample.

The researchers have explored the main factors which can cause a deviation in the oil–paper insulation’s FDS data, such as the testing temperature, the geometry structure of power equipment, and the noise in the testing environment. In reference [100], based on the Arrhenius theory, the main curve technology has been adopted to eliminate the influence of the testing temperature on FDS data. In reference [101], the XY model has been used to correct the effect of geometry structure on the FDS testing results and obtain the pure oil–paper insulation’s FDS data. To reduce the influence of noise and enhance the anti-interference ability of the FDS testing, the higher-level voltage is usually selected as the AC excitation voltage in field testing.

5.2. Extraction of the Dielectric Response Feature Parameters

According to the existing research, there is rich oil–paper insulation information existing in the FDS curve. Thus, it is critical and significant to extract the feature parameters from the FDS curve, which are related to the insulating state (aging degree and moisture content) of oil–paper insulation. Currently, there are three common methods to extract the feature parameters from the FDS curve: (1) extracting the shape characteristics and

geometric parameters of the FDS curve, (2) processing the FDS curve based on the mathematical methods, and (3) fitting the FDS curve based on the frequency dielectric equivalent circuit models.

5.2.1. Extracting the Shape Characteristics and Geometric Parameters of the FDS Curve

Considering that the FDS curve has an obvious frequency dependence, while the oil–paper insulation has a serious aging state or high moisture content, there is an obvious loss peak existing in the FDS curve of oil–paper insulation. Meanwhile, the amplitude value of this loss peak and the corresponding frequency can be adopted as the feature parameters to reflect the aging degree and moisture content of the oil–paper insulation. In reference [102], the quantitative relationship between the minimum value of the dielectric loss factor and the oil–paper insulation’s moisture content have been established. Fan et al. have obtained the dielectric loss factor curves of the oil–paper insulation with various aging degrees and moisture contents, and the integral values of the dielectric loss factor curve at different frequency intervals (such as 10^{-3} – 10^{-2} , 10^{-2} – 10^{-1} , 10^2 – 10^3) have been calculated as feature parameters [103]. Then, the insulation state evaluation model has been established to evaluate the oil–paper insulation’s aging degrees and moisture contents, and the accuracy of this model has been verified by field testing.

The above methods can extract the feature parameters which can reflect the aging degree and moisture content of the oil–paper insulation rapidly and easily. However, the insulation information of these feature parameters is insufficient, and it is difficult to obtain universal conclusions based on these feature parameters. Meanwhile, these feature parameters are seriously affected by the FDS testing conditions, such as the testing temperature and the electromagnetic noise. Thus, this method cannot be adopted widely in field testing.

5.2.2. Processing the FDS Curve Based on the Mathematical Methods

While the researchers extract the shape characteristics of the FDS curve, the specific frequencies are chosen based on the personal experience of the researchers. This method has been limited by subjective factors without a clear dielectric response theory. Thus, the extracted feature parameters are not reliable for studying the practical dielectric response processes in oil–paper insulation. To address this issue, mathematical and physical theories are introduced to process the FDS data and change the shape of the FDS curve. Then, FDS data with more obvious features and more clear meanings are obtained. The above mathematical and physical theories mainly include the FDS curve integral method [104], dielectric modulus method [105], and logarithmic derivative spectral method [106], shown in Table 3.

Fan et al. have extracted the feature parameters based on the FDS curve integral method and established the quantitative relationships between the extracted feature parameters and the oil–paper insulation’s aging degree [104]. The dielectric modulus has been defined as the inverse of $\varepsilon^*(\omega)$ [105]. The dielectric modulus method can not only uncover the oil–paper insulation’s dielectric response processes but also highlight the polarization information at the low-frequency regions of the FDS curve. In reference [107], the feature parameters have been extracted based on the dielectric modulus method. Then, the moisture content of the oil–paper insulation has been evaluated based on the above feature parameters and machine learning technology. However, the dielectric modulus method can only reduce or restrain the influence of the conductance effect on the polarization information, rather than eliminate its effect. To obtain the pure polarization information, the logarithmic derivative spectral method has been proposed. In reference [106], the polarization information has been extracted based on the logarithmic derivative spectral method, and the correlation between the extracted polarization information and the oil–paper insulation’s aging degree has been proved.

Table 3. Illustration of data processing methods and corresponding equations.

Method	Equation	Illustration
integral spectrum	$\begin{cases} F_1 = \int_a^b \tan\delta(\omega) d\omega \\ F_2 = \int_a^b \epsilon'(\omega) d\omega \\ F_3 = \int_a^b \epsilon''(\omega) d\omega \end{cases}$	
dielectric modulus	$\begin{cases} M'(\omega) = \frac{\epsilon'(\omega)}{\epsilon'(\omega)^2 + \epsilon''(\omega)^2} \\ M''(\omega) = \frac{\epsilon''(\omega)}{\epsilon'(\omega)^2 + \epsilon''(\omega)^2} \end{cases}$	
Logarithmic derivative spectroscopy	$\begin{cases} \Phi_{real}(\omega) = -\frac{\partial \epsilon_{tot}'(\omega)}{\partial \ln(\omega)} \\ \Phi_{imag}(\omega) = -\frac{\partial \epsilon_{tot}''(\omega)}{\partial \ln(\omega)} \end{cases}$	

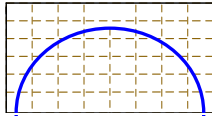
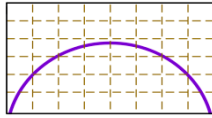
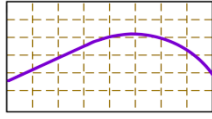
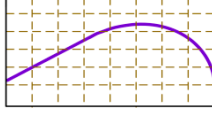
5.2.3. Fitting the FDS Curve Based on the Frequency Dielectric Equivalent Circuit Models

Considering that the feature parameters extracted in Sections 5.2.1 and 5.2.2 have no practical physical meaning, these feature parameters are not reliable for researching the microphysical mechanism of the complex dielectric responses during the oil–paper insulation’s aging and dampness. To address this issue, many equivalent circuit models have been proposed to simulate the FDS data of the oil–paper insulation system, which includes the Debye model [108], Cole–Cole model [109], Davidson–Cole model [110], and Havriliak–Negami model [111] in Table 4.

In the Debye model, the dielectric response has been simulated by the combination of a capacitor and a resistor [108]. However, the Debye model considers there is only a single dielectric response process in oil–paper insulation, which is not practical. Thus, the Cole–Cole model has been proposed to simulate more complex dielectric response processes by multiple combinations of capacitors and resistors. In reference [109], the feature parameters in the Cole–Cole model have been extracted from the FDS data, and the oil–paper insulation’s aging state has been evaluated based on these feature parameters. However, the multiple combinations of capacitors and resistors can only reflect the ideal dielectric response processes, which correspond to the half-circuit in the complex plane. Thus, the distribution parameters (i.e., α and β) in the Davidson–Cole model and the Havriliak–Negami model have been adopted to correct the Cole–Cole model. Then, it has been proved that the circuit components in these models contain the polarization information and conduction information of the dielectric response processes in the oil–paper insulation. In reference [112], the correlation between the feature parameters in the above equivalent circuit models and the oil–paper insulation’s insulating state has been proved and analyzed. Further, the aging state and moisture content of the oil–paper

insulation can be evaluated accurately based on the above feature parameters and machine learning technology.

Table 4. Equivalent circuit models and corresponding complex plane.

Model	Math Expression	Complex Plane
Debye Model	$\varepsilon^*(w) = \varepsilon_\infty + \frac{\varepsilon_s - \varepsilon_\infty}{1 + j \cdot w \tau}$	
Cole–Cole Model	$\varepsilon^*(w) = \varepsilon_\infty + \frac{\varepsilon_s - \varepsilon_\infty}{1 + (j \cdot w \tau)^{1-\alpha}}$ ($0 < \alpha < 1$)	
Davidson–Cole Model	$\varepsilon^*(w) = \varepsilon_\infty + \frac{\varepsilon_s - \varepsilon_\infty}{(1 + j \cdot w \tau)^\beta}$ ($0 < \beta < 1$)	
Havriliak–Negami Model	$\varepsilon^*(w) = \varepsilon_\infty + \frac{\varepsilon_s - \varepsilon_\infty}{[1 + (j \cdot w \tau)^{1-\alpha}]^\beta}$ ($0 < \alpha < 1, 0 < \beta < 1$)	

5.3. Assessment of the Aging Degree and Moisture Content

Reviewing the existing research [113], there are multiple methods that have been adopted to obtain feature parameters (such as the content of chemical indicators, infrared spectral properties, and dielectric response parameters), which are related to the aging degree and moisture content of the oil–paper insulation. Thus, based on the extracted feature parameters, the next work will focus on proposing reliable techniques for evaluating the aging degree and moisture content of oil–paper insulation. One such assessment approach involves initially, preparing the oil–paper insulation samples with various aging degrees and moisture contents in a laboratory and then obtaining the feature parameters for each insulation state. Finally, with curve or surface fitting techniques, one must establish the quantitative relationships between the insulation states and extracted feature parameters, thereby facilitating the insulation states evaluation. An alternative assessment method consists of first constructing the feature parameters/insulation states database with interpolation methods, data augmentation techniques, or generative adversarial networks based on the above insulation states and their corresponding feature parameters and secondly, proposing an insulation state classification model based on machine learning algorithms. Finally, one must train and optimize the classification model using the constructed database to achieve the accurate insulation states evaluation.

5.3.1. Insulation States Evaluation Using Curve and Surface Fitting Techniques

After acquiring the feature parameters related to aging state and moisture content from dielectric response data, researchers analyze the changing trends of these parameters in relation to DP and moisture content to ascertain any correlations. For the feature parameters which exhibit a strong correlation with the insulation state, curve and surface fitting techniques are employed to derive quantitative equations between them and DP/mc%, thereby evaluating the insulation state of the oil–paper system. In reference [114], by comparing the PDC properties of natural ester–paper insulation samples and mineral oil–paper insulation samples during the aging process, an exponential relation between the stable depolarization charge quantity and the insulating paper’s DP has been proposed. By analyzing the FDS data of oil–paper insulations under various moisture contents, a new frequency dielectric feature parameter for evaluating the oil–paper insulation’s

moisture content has been proposed [115]. Further, the improved Cole–Cole model is adopted to extract the feature parameters (α relaxation components, dc, and hopping conductivity components) from FDS data [116]. Then, the quantitative equations between the above parameters and the oil–paper insulation’s DP are obtained. In reference [117], the feature parameters (distribution parameter β and relaxation time τ) are proposed from the Davidson–Cole model, and the quantitative relationships between the feature parameters and DP, as shown in Equation (21), are adopted to evaluate the oil–paper insulation’s aging state.

$$\begin{cases} \beta = -1.122 \times \exp(-DP/3.120) + 0.921 \\ \Delta\varepsilon = 185.208 \times \exp(-DP/474.770) - 18.157 \\ \tau = -27851.426 \times \exp(-DP/377.400) + 6178.100 \end{cases} \quad (21)$$

In the above equations, β is the distribution parameter in the Davidson–Cole model, and $\Delta\varepsilon$ is the difference between the static dielectric constant ε_s and the optical frequency dielectric constant ε_∞ of the sample ($\varepsilon_s - \varepsilon_\infty$). T represents the relaxation time of the dielectric medium.

5.3.2. Insulation States Evaluation Using Machine Learning Techniques

The above methods demand a high level of technical expertise and detailed understanding of the technique. Furthermore, similar evaluations require repetitive calculations to analyze different subjects, making the process not only inefficient and time-consuming but also complex and cumbersome, thereby limiting its applicability and widespread adoption. Machine learning algorithms can derive insights from existing data and uncover patterns hidden within. By continuously learning from a feature parameters/insulation states database, machine learning accumulates experience and ultimately applies this knowledge for accurate assessments of the oil–paper insulation’s aging state and moisture content, as shown in Figure 15. In reference [118], the Raman spectra of the insulating oil have been collected in the range from 400 cm^{-1} to 3000 cm^{-1} , and the Voigt function has been adopted to obtain the feature parameters from the measured Raman spectra. Then, the support vector machine has been adopted to evaluate the aging state of oil–paper insulation. Further [119], the Raman spectra and support vector machine have been adopted to evaluate the aging state of the oil–paper insulation with different oil–paper ratios. Atefeh et al. have adopted the ratio of gaseous compounds dissolved in the insulating oil as the feature parameters, and the fuzzy support vector machine has been adopted to evaluate the synthesized health condition of the oil–paper insulation [120]. Fan et al. have adopted the dielectric modulus method to extract the feature parameters from the oil–paper insulation’s FDS data. Then, the oil–paper insulation’s moisture content has been evaluated by the genetic algorithm/improved support vector machine [121].

Yi Cui et al. have collected various insulating oil characteristic datasets from different utility companies and adopted the KNN to evaluate the oil–paper insulation’s aging state [122]. In reference [123], the KNN has been adopted to identify the insulation state of insulating paper and the accuracy of the recognition results is satisfactory. Fan et al. have extracted the dielectric feature parameters with the logarithmic derivative spectral method, and the evaluation model of the oil–paper insulation’s moisture content has been established based on the KNN algorithm [124]. In reference [125], the fingerprint database has been established based on the dielectric feature parameters, and the aging degree and moisture content of the oil–paper insulation have been evaluated with the weighted k-nearest neighbor regression. In reference [126], the moisture content in the insulating oil has been evaluated based on the BPNN, whose weights and biases have been improved by the genetic algorithm (GA). Zhuang et al. have established the fingerprint database based on the feature parameters, which are the resistivity of oil–paper insulation’s different regions and the dielectric loss factor. Then, the aging degree of the oil–paper insulation has been evaluated accurately based on the above fingerprint database and the BPNN [127]. Ding et al. have extracted the feature parameters from oil–paper insulation’s FDS data by the logarithmic derivative spectral method, which are related to the aging degree and

moisture content of the oil–paper insulation. Then, the condition assessment model has been established based on the back propagation neural network, which has been modified by the adaptive boosting algorithm [128].

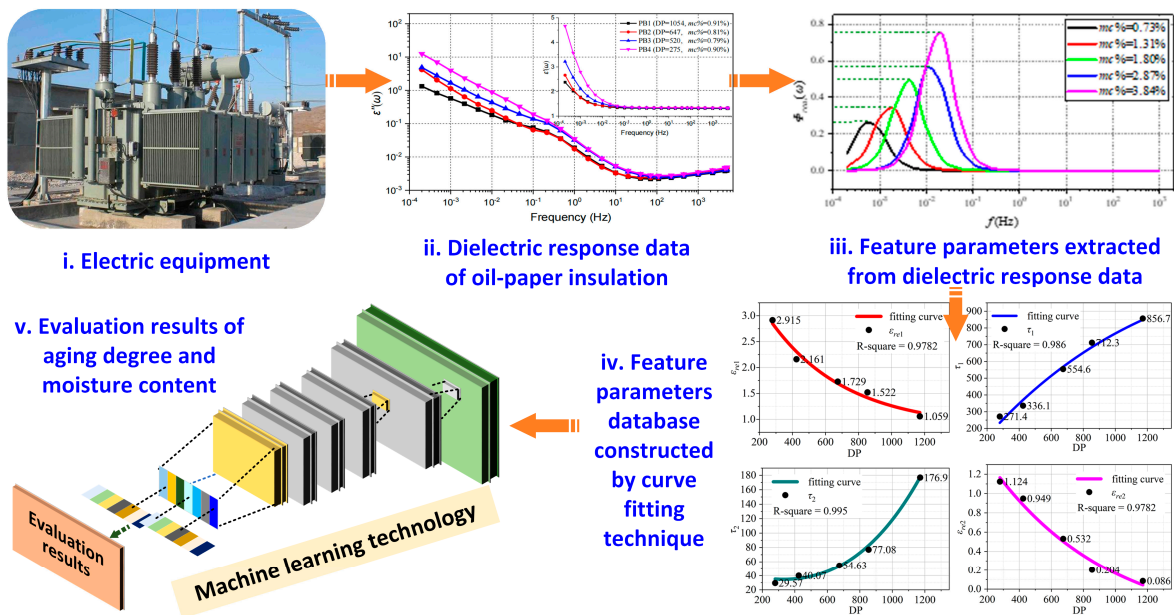


Figure 15. A schematic diagram of oil–paper insulation states evaluation with machine learning technology.

6. Prospects for the Future Research

6.1. Research on Hotspots' Oil–Paper Insulation System

6.1.1. The Engineering Significance of the Hotspot Research

The existing research focuses on studying the aging degree and moisture content of oil–paper insulation, which ages under a uniform temperature field. However, due to the geometrical structure of the power equipment and the circulation flow of insulating oil, the temperature distribution in the power equipment is non-uniform [129]. Specifically, the above temperature distribution follows the principles of being proportional to insulation height and inversely proportional to insulation distance. The temperature distribution of transformer oil–paper insulation is shown in Figure 16 as an example. Thus, the oil–paper insulation in different regions ages under different temperatures. In summary, the aging degree and moisture content of each region's oil–paper insulation is different.

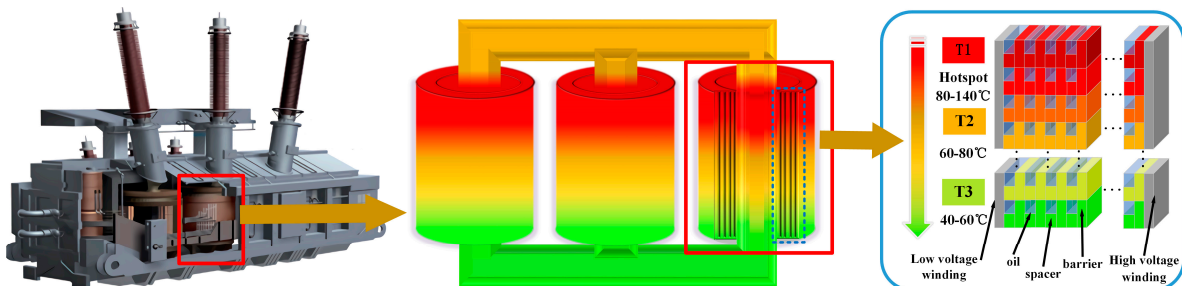


Figure 16. A schematic diagram of temperature distribution of transformer oil–paper insulation.

Reviewing the existing research [130], the oil–paper insulation at the highest temperature region (i.e., hotspot) has the most serious aging degree. Thus, the oil–paper insulation at the hotspot will gradually develop to be the weakest point of the whole oil–paper insulation system. Considering the ‘shortboard effect’, the insulation performance and service

life of the in-service oil–paper insulation are determined by the insulation level of the hotspot’s oil–paper insulation. Thus, it is necessary and significant to obtain the feature parameters related to the insulation state of the hotspot’s oil–paper insulation and research the quantitative relationship between the above feature parameters and the insulation state of the hotspot’s oil–paper insulation. Based on the above quantitative relationship, the feature parameters database can be established and a state assessment can be proposed to evaluate the aging degree and moisture content of the oil–paper insulation at the power equipment’s hotspot.

6.1.2. Existing Results of Hotspot Research

Reviewing the existing research, researchers have made numerous valuable attempts at non-uniform aging of oil–paper insulation, as a study on chemical indicators and electrical parameters. In reference [131], it has been proved that there is a correlation between the methanol content in insulating oil and the aging degree of the hotspot’s oil–paper insulation. Further, Zhang et al. have analyzed the correlation between the methanol content and the hotspot’s temperature and proven that the distribution of methanol in the axial direction is non-uniform [132]. In reference [133], an equation between the aging degree of the hotspot’s oil–paper insulation and the concentration of the 2-FAL dissolved in the insulating oil has been established, as shown in Equation (22). The effectiveness and reliability of the above equation have been verified based on the non-uniform thermal aging experiment.

$$C_{oil}(t) = \int_0^1 \left(\frac{1}{DP_{min}} - \frac{1}{DP_0} \right) \cdot \frac{1}{kV_{oil}} \cdot w_{oil}[T(h), H(h), DP(h)] \cdot e^{\frac{E_a}{R \cdot [T_{max} + 273]} - \frac{E_a}{R \cdot [T(h) + 273]}} dh \quad (22)$$

In the above equations, $C_{oil}(t)$ represents the concentration of 2-FAL dissolved in oil, and DP_{min} represents the aging degree of insulation paper during testing. DP_0 represents the initial DP value of the insulating paper. k is a constant that depends on the initial state of the insulating paper and V_{oil} represents the volume of insulating oil. $T(h)$, $H(h)$, and $DP(h)$ are the temperature distribution function of the windings, the moisture distribution function of the paper insulation of the windings, and the DP value distribution function of the transformer as the height changes, respectively. E_a is the activation energy of the insulating paper and its value is 11,000 J/mol. R is the gas constant with a value of 8.314 J/(mol·k). T_{max} represents the maximum value of the winding temperature.

As for the study on electrical parameters, in reference [134], the influence of the non-uniform aging situation and the non-uniform moisture distribution on the oil–paper insulation’s FDS data has been researched. Meanwhile, the microscopic mechanism of dielectric response processes during the non-uniform aging process has been discussed. Reference [135] has revealed that the peak, steady-state values and integral of the polarization current are negatively correlated with the location of the wettest insulation layer and positively correlated with the moisture content of the wettest layer. The position of the wettest layer in radially non-uniform damp bushings can be determined by the difference in polarization current integrals under positive and negative PDC connections. Sun et al. have proposed a modified simulation model based on the finite element method and the improved XY model, which is adopted to simulate the dielectric response data of the non-uniform aging oil–paper insulation. Meanwhile, the effectiveness of the proposed model has been verified [136]. Further [137], Wang et al. have adopted the artificial intelligence optimization algorithm to search for the optimal parameters in the above simulation model, which can accurately simulate the FDS data of the non-uniform aging oil–paper insulation. Then, the quantitative relationship between the obtained parameters and the DP of the hotspot’s insulating paper has been proposed.

Considering that the traditional equivalent circuit models are only effective for researching the dielectric response data of the uniform aging of oil–paper insulation, in reference [138], the modified Debye model has been proposed to simulate the polarization and depolarization currents (PDC data) of the non-uniform aging of oil–paper insulation. It has been proved that the feature parameters (such as pole value and zero value of the

modified Debye model's transfer function) are effective for researching the non-uniform aging of oil–paper insulation. Fan et al. have proposed the modified XY model as shown in Equation (23) to decouple the hotspot's FDS data from the whole oil–paper insulation's FDS data, and the non-dominated sorting genetic algorithm (NSGA) has been adopted to search for the optimal feature parameters in the modified XY model [139].

$$\varepsilon_{tot}^*(\omega) = \zeta^*(\omega) \cdot \left[\frac{mY}{\sum_{i=1}^m \frac{1}{\varepsilon_{rpi}^*(\omega)}} + \frac{1-Y}{\frac{1-X}{\varepsilon_{ro}(\omega)} + \frac{X}{m} \left(\sum_{i=1}^m \frac{1}{\varepsilon_{rpi}^*(\omega)} \right)} \right] \quad (23)$$

In the above equations, ζ is the response parameter. X and Y are the geometric parameters of the insulation system. In this model, it is necessary to assume that the FDS data for the hotspot area are known and then invert the FDS data for the overall insulation system. In such a case, the NSGA can be used to accurately search for the best feature parameters in the improved XY model.

6.1.3. Potential Issues with Hotspot Research

Reviewing the existing research, the correlation between the concentration of the chemical indicators dissolved in the insulating oil and the aging state of the hotspot's oil–paper insulation has been proved. However, the quantitative relationship between the concentration of the above chemical indicators and the insulation state (aging degree and moisture content) of the hotspot's oil–paper insulation has not been found. Meanwhile, the extraction method of dielectric feature parameters is based on simulating the whole oil–paper insulation's FDS data with intelligent algorithms. This method can only satisfy the accuracy in the mathematical sense, and the extracted feature parameters do not have practical physical significance. Thus, it is necessary to search for the feature parameters based on the comprehensive consideration of mathematical accuracy and dielectric significance.

The existing research focuses on obtaining the chemical and dielectric feature parameters, which are related to the insulation state of the hotspot's oil–paper insulation. In future work, it is necessary and meaningful to prepare more non-uniform aging oil–paper insulation samples and establish the feature parameters fingerprint database. The machine learning techniques have full potential for establishing the condition assessment model and achieving the accurate evaluation of the hotspot's insulation state (aging degree and moisture content).

6.2. Research on the Joint Evaluation Technique of Electrical–Chemical Feature Parameters

6.2.1. The Engineering Significance of the Joint Evaluation Technique

According to the existing research [140], the chemical indicators and electrical parameters can both be adopted to research the aging degree and moisture content of the oil–paper insulation. However, there are some limitations to the application of the two methods. The chemical indicators dissolved in the insulating oil can be lost during the operation of oil flowing and oil filtrating, causing an error in evaluating the aging state of the oil–paper insulation. The electrical parameters have similar change laws, with the oil–paper insulation's aging degree and moisture content increasing. Due to the complementary effect of the aging degree and moisture content, it is difficult to accurately evaluate the aging degree and moisture content of the oil–paper insulation samples while they are both unknown. Thus, based on the great sensitivity of the chemical indicators to the aging degree and the overall advantage of the electrical parameters to the entire insulation state, the joint evaluation technique of electrical–chemical feature parameters has been proposed to evaluate the aging degree and moisture content of the oil–paper insulation.

6.2.2. Existing Results on the Joint Evaluation Technique

In reference [141], the change laws of the chemical indicators during the oil–paper insulation's aging process have been revealed in detail. Specifically, with the oil–paper in-

sulation's aging degree increasing, the contents of the small molecule compounds (furfural, alcohols, and acids) dissolved in the insulating oil increase gradually. In reference [142], the dielectric response performances of the oil–paper insulation system with various aging degrees and moisture contents have been researched. With the oil–paper insulation's aging degree and moisture content increasing, the dielectric loss factor and DC conductivity increase gradually, and the electrical breakdown strength decreases. Teymouri et al. have proposed a mathematical empirical equation for calculating the activation energy of the aging reaction. Then, based on the calculated activation energy, a novel life management model for the oil–paper insulation system has been proposed, which consists of the chemical aging model and the electrical–thermal aging model [143].

6.2.3. Potential Issues of the Joint Evaluation Technique

Considering that the chemical and electrical feature parameters are inputted in the joint evaluation technique simultaneously, which can cause an obvious increase in the complexity and dimension of the input data, it is critical for the joint evaluation technique to improve the ability to process the complex input data and uncover the effective feature information. Reviewing the existing research [144], deep learning techniques are effective methods to reduce the dimension of input data and extract low-dimensional feature information, such as a convolutional neural network (CNN), recursive neural network (RNN), and generative adversarial network (GAN). Thus, deep learning has full potential for establishing a joint evaluation model for researching the aging degree and moisture content of the oil–paper insulation system.

7. Conclusions

In this work, various techniques for evaluating the aging degree and moisture content of the oil–paper insulation system have been introduced and discussed. The core principle of the condition assessment techniques is obtaining the feature parameters, which are related to the aging degree and moisture content of the oil–paper insulation system. Then, the insulation state evaluation models can be established based on the obtained feature parameters and machine learning techniques. This work has the following conclusions.

- I. The oil–paper insulation system in the power equipment is made up of insulating paper and insulating oil, and the geometry structure of the oil–paper insulation has been shown in Section 2. Also, the preparation process and microscopic structure of the insulating paper and insulating oil have been introduced. Meanwhile, the internal reason for the great insulation performance of the oil–paper insulation has been revealed. Finally, the main reasons for and forms of the oil–paper insulation's degradation process have been discussed.
- II. The techniques for evaluating the oil–paper insulation's aging degree and moisture content have been reported in Sections 3 and 4, respectively. These techniques can be divided into destructive techniques (such as DP and TS testing) and non-destructive techniques (such as chemical indicators testing). Meanwhile, they can be divided into direct measurement techniques (such as the Karl Fischer titration technique) and indirect calculation techniques (such as the cellulose–water adsorption isotherm technique). The technical principles of these techniques have been introduced, and the development process and research results of these techniques have been reported in detail. Finally, the main advantages and limitations of these techniques have been discussed and analyzed.
- III. The techniques introduced in Sections 3 and 4 are only effective for evaluating a single insulation state (aging degree and moisture content) of oil–paper insulation. However, the dielectric response technique introduced in Section 5 can be adopted to evaluate the aging degree and moisture content of oil–paper insulation simultaneously. The whole evaluation process based on the dielectric response technique can be divided into three parts: (1) collecting the dielectric response data of oil–paper insulation (RVM, PDC, and FDS), (2) extracting the feature parameters

from the collected dielectric response data, which are related to the aging degree and moisture content of the oil–paper insulation, and (3) establishing insulation state evaluation models based on the curve/surface fitting techniques and machine learning techniques.

- IV. Two full potential topics have been introduced in Section 6, which are research on hotspots’ oil–paper insulation systems and research on the joint evaluation technique of electrical–chemical feature parameters. The existing research on the hotspot focuses on the extraction of feature parameters, which can reflect the aging degree and moisture content of the hotspot’s oil–paper insulation. In future work, it is important to reveal the practical physical meaning of the extracted feature parameters and establish an insulation state evaluation model for the hotspot’s oil–paper insulation. As for the electrical–chemical joint evaluation technique, it is critical to improve its ability to process complex input data and uncover effective feature information, so a deep learning technique is an ideal choice.

Author Contributions: In this research activity, X.L. edited Section 1; H.Z. edited Section 2; E.Z. edited Section 3; Z.J. edited Sections 4 and 5; C.L. edited Section 6; J.L. checked the manuscript; X.F. is the corresponding author. All authors have read and agreed to the published version of the manuscript.

Funding: This work was supported in part by the National Natural Science Foundation of Beijing under Grant 3244048 and in part by the 2023 National Postdoctoral Research Program under Grant GZC20231210.

Conflicts of Interest: Author Xin Li was employed by the company State Grid Sichuan Electric Power Company Ultra High Voltage Branch. The remaining authors declare that the research was conducted in the absence of any commercial or financial relationships that could be construed as a potential conflict of interest.

References

- Shu, Y.; Chen, W. Research and application of UHV power transmission in China. *High Volt.* **2018**, *3*, 1–13. [\[CrossRef\]](#)
- Tenbohlen, S.; Coenen, S.; Djamali, M.; Müller, A.; Samimi, M.H.; Siegel, M. Diagnostic measurements for power transformers. *Energies* **2016**, *9*, 347. [\[CrossRef\]](#)
- Wang, M.; Vandermaar, A.J.; Srivastava, K.D. Review of condition assessment of power transformers in service. *IEEE Electr. Insul. Mag.* **2002**, *18*, 12–25. [\[CrossRef\]](#)
- Li, S.; Li, J. Condition monitoring and diagnosis of power equipment: Review and prospective. *High Volt.* **2017**, *2*, 82–91. [\[CrossRef\]](#)
- Liao, R.; Liu, J.; Yang, L.; Wang, K.; Hao, J.; Ma, Z.; Gao, J.; Lv, Y. Quantitative analysis of insulation condition of oil-paper insulation based on frequency domain spectroscopy. *IEEE Trans. Dielectr. Electr. Insul.* **2015**, *22*, 322–334. [\[CrossRef\]](#)
- Tang, C.; Huang, B.; Hao, M.; Xu, Z.; Hao, J.; Chen, G. Progress of space charge research on oil-paper insulation using pulsed electroacoustic techniques. *Energies* **2016**, *9*, 53. [\[CrossRef\]](#)
- Liao, R.; Yang, L.; Li, J.; Grzybowski, S. Aging condition assessment of transformer oil-paper insulation model based on partial discharge analysis. *IEEE Trans. Dielectr. Electr. Insul.* **2011**, *18*, 303–311. [\[CrossRef\]](#)
- Song, R.; Chen, W.; Yang, D.; Zhang, R.; Wang, Z. Aging assessment of oil–paper insulation based on visional recognition of the dimensional expanded Raman spectra. *IEEE Trans. Instrum. Meas.* **2021**, *70*, 1–10. [\[CrossRef\]](#)
- Dong, M.; Ren, M.; Wen, F.; Zhang, C.; Liu, J. Explanation and analysis of oil-paper insulation based on frequency-domain dielectric spectroscopy. *IEEE Trans. Dielectr. Electr. Insul.* **2015**, *22*, 2684–2693. [\[CrossRef\]](#)
- Przybyłek, P. The influence of temperature and aging of cellulose on water distribution in oil-paper insulation. *IEEE Trans. Dielectr. Electr. Insul.* **2013**, *20*, 552–556. [\[CrossRef\]](#)
- Zhang, E.; Liu, J.; Zhang, C.; Zheng, P.; Nakanishi, Y.; Wu, T. State-of-Art Review on Chemical Indicators for Monitoring the Aging Status of Oil-Immersed Transformer Paper Insulation. *Energies* **2023**, *16*, 1396. [\[CrossRef\]](#)
- Yan, J.; Liao, R.; Yang, L.; Li, J. Study on microstructure and electrical properties of oil-impregnated paper insulation after exposure to partial discharge. *Eur. Trans. Electr. Power* **2012**, *22*, 733–746. [\[CrossRef\]](#)
- Mo, Y.; Yang, L.; Hou, W.; Zou, T.; Huang, Y.; Zheng, X.; Liao, R. Preparation of cellulose insulating paper of low dielectric constant by OAPS grafting. *Cellulose* **2019**, *26*, 7451–7468. [\[CrossRef\]](#)
- Jalbert, J.; Rodriguez-Celis, E.M.; Arroyo-Fernández, O.H.; Duchesne, S.; Morin, B. Methanol marker for the detection of insulating paper degradation in transformer insulating oil. *Energies* **2019**, *12*, 3969. [\[CrossRef\]](#)
- Okabe, S.; Kaneko, S.; Kohtoh, M.; Amimoto, T. Analysis results for insulating oil components in field transformers. *IEEE Trans. Dielectr. Electr. Insul.* **2010**, *17*, 302–311. [\[CrossRef\]](#)

16. Wang, X.; Tang, C.; Huang, B.; Hao, J.; Chen, G. Review of research progress on the electrical properties and modification of mineral insulating oils used in power transformers. *Energies* **2018**, *11*, 487. [[CrossRef](#)]
17. Han, S.; Li, Q.; Li, C.; Yan, J. Electrical and mechanical properties of the oil-paper insulation under stress of the hot spot temperature. *IEEE Trans. Dielectr. Electr. Insul.* **2014**, *21*, 179–185. [[CrossRef](#)]
18. He, Y.; Yang, L.; Cheng, L.; Chen, Q.; Yu, H.; Hou, W. Cellulose hydrogen bond detection using terahertz time-domain spectroscopy to indicate deterioration of oil–paper insulation. *Cellulose* **2023**, *30*, 727–740. [[CrossRef](#)]
19. Zhou, Y.; Huang, M.; Chen, W.; Lu, L.; Jin, F.; Huang, J. Space charge behavior evolution with thermal aging of oil-paper insulation. *IEEE Trans. Dielectr. Electr. Insul.* **2015**, *22*, 1381–1388. [[CrossRef](#)]
20. Zhou, L.J.; Wu, G.N.; Liu, J. Modeling of transient moisture equilibrium in oil-paper insulation. *IEEE Trans. Dielectr. Electr. Insul.* **2008**, *15*, 872–878. [[CrossRef](#)]
21. Batra, P.E.; Ioannides, M.G. Assessment of Electric Accidents in Power Industry. *Hum. Factors Ergon. Manuf.* **2002**, *10*, 1002. [[CrossRef](#)]
22. Zhang, X.; Ren, L.; Yu, H.; Xu, Y.; Lei, Q.; Li, X.; Han, B. Dual-Temperature Evaluation of a High-Temperature Insulation System for Liquid-Immersed Transformer. *Energies* **2018**, *11*, 1957. [[CrossRef](#)]
23. Vasovic, V.; Lukic, J.; Mihajlovic, D.; Pejovic, B.; Radakovic, Z.; Radoman, U.; Orlovic, A. Aging of transformer insulation—Experimental transformers and laboratory models with different moisture contents: Part I—DP and furans aging profiles. *IEEE Trans. Dielectr. Electr. Insul.* **2019**, *26*, 1840–1846. [[CrossRef](#)]
24. Ekenstam, A. The behavior of cellulose in mineral acid solutions: Kinetics study of the decomposition of cellulose in acid solutions. *Ber* **1936**, *69*, 540–553.
25. Peng, L.; Fu, Q.; Li, L.; Lin, M. Indirect detection of DP for insulating paper based on methanol content in transformer oil by spectroscopic approach. *IEEE Trans. Dielectr. Electr. Insul.* **2019**, *26*, 90–94. [[CrossRef](#)]
26. Arroyo, O.H.; Jalbert, J.; Fofana, I.; Ryadi, M. Temperature dependence of methanol and the tensile strength of insulation paper: Kinetics of the changes of mechanical properties during ageing. *Cellulose* **2017**, *24*, 1031–1039. [[CrossRef](#)]
27. Hill, D.J.T.; Le, T.T.; Darveniza, M. A study of degradation of cellulosic insulation materials in a power transformer. Part 2: Tensile strength of cellulose insulation paper. *Polym. Degrad. Stab.* **1995**, *49*, 429–435. [[CrossRef](#)]
28. N’cho, J.S.; Fofana, I.; Hadjadj, Y.; Beroual, A. Review of physicochemical-based diagnostic techniques for assessing insulation condition in aged transformers. *Energies* **2016**, *9*, 367. [[CrossRef](#)]
29. *IEEE Std C57.104-1991*; IEEE Guide for the Interpretation of Gases Generated in Oil-Immersed Transformers. IEEE: New York, NY, USA, 1992.
30. *IEC 60599-1999*; Mineral Oil-filled Electrical Equipment in Service-Guidance on the Interpretation of Dissolved and Free Cases. IEC: New York, NY, USA, 1999.
31. Rogers, R.R. IEEE and IEC codes to interpret incipient faults in transformers, using gas in oil analysis. *IEEE Trans. Dielectr. Electr. Insul.* **1978**, *EI-13*, 349–354. [[CrossRef](#)]
32. Duval, M.; DePabla, A. Interpretation of gas-in-oil analysis using new IEC publication 60599 and IEC TC 10 databases. *IEEE Electr. Insul. Mag.* **2001**, *17*, 31–41. [[CrossRef](#)]
33. Tamura, R.; Anetai, H.; Ishii, T. The diagnosis on the aging deterioration of insulating paper in transformers by gas analysis. *Trans. Inst. Electr. Eng.* **1981**, *101*, 30–36.
34. Lelekakis, N.; Martin, D.; Guo, W.; Wijaya, J. Comparison of dissolved gas-in-oil analysis methods using a dissolved gas-in-oil standard. *IEEE Electr. Insul. Mag.* **2011**, *27*, 29–35. [[CrossRef](#)]
35. Matharage, S.; Liu, Q.; Wang, Z.; Wilson, G.; Krause, C. Aging assessment of synthetic ester impregnated thermally non-upgraded kraft paper through chemical markers in oil. *IEEE Trans. Dielectr. Electr. Insul.* **2018**, *25*, 507–515. [[CrossRef](#)]
36. Lin, Y.; Wei, C.; Tao, F.; Li, J. Aging assessment of oil-paper insulation of power equipment with furfural analysis based on furfural generation and partitioning. *IEEE Trans. Power Deliv.* **2019**, *34*, 1626–1633. [[CrossRef](#)]
37. Zhang, Z.; Cheng, D.; Xu, H.; Wu, Y.; Fan, J. Bioactivities and mechanism of spiro enol ether analogues against *Pieris rapae*. *Insect Sci.* **2004**, *11*, 19–26. [[CrossRef](#)]
38. Es-Safi, N.E.; Cheynier, V.; Moutounet, M. Study of the reactions between (+)-catechin and furfural derivatives in the presence or absence of anthocyanins and their implication in food color change. *J. Agric. Food Chem.* **2000**, *48*, 5946–5954. [[CrossRef](#)]
39. Liu, J.; Song, B.; Zhang, E.; Zhang, H.; Zhang, Y.; Goh, H.H. Two-stage Residual Lifespan Prediction Model for Oil-paper Insulation Based on Analysis of Furfural and Methanol in Oil. *IEEE Trans. Power Deliv.* **2022**, *38*, 432–441. [[CrossRef](#)]
40. *DL/T596-1996*; Preventive Test for Electric Power Equipment. National Energy Administration: Wuhan, China, 1996.
41. Hao, J.; Feng, D.; Liao, R.; Yang, L.; Lin, Y. Effect of temperature on the production and diffusion behaviour of furfural in oil–paper insulation systems. *IET Gener. Transm. Distrib.* **2018**, *12*, 3124–3129. [[CrossRef](#)]
42. Jalbert, J.; Gilbert, R.; Tétreault, P.; Morin, B.; Lessard-Déziel, D. Identification of a chemical indicator of the rupture of 1,4- β -glycosidic bonds of cellulose in an oil-impregnated insulating paper system. *Cellulose* **2007**, *14*, 295–309. [[CrossRef](#)]
43. Matharage, S.; Liu, Q.; Wang, Z. Aging assessment of kraft paper insulation through methanol in oil measurement. *IEEE Trans. Dielectr. Electr. Insul.* **2016**, *23*, 1589–1596. [[CrossRef](#)]
44. Zheng, H.; Shi, K.; Yang, T.; Li, Y.; Zhang, E.; Zhang, C.; Shao, G.; Shi, Z.; Zhang, C. Investigation on the equilibrium distribution of methanol in transformer oil-immersed cellulosic insulation. *Cellulose* **2021**, *28*, 1703–1714. [[CrossRef](#)]

45. Schaut, A.; Autru, S.; Eeckhoudt, S. Applicability of methanol as new marker for paper degradation in power transformers. *IEEE Trans. Dielectr. Electr. Insul.* **2011**, *18*, 533–540. [[CrossRef](#)]
46. Laurichesse, D.; Bertrand, Y.; Tran-Duy, C.; Murin, V. Ageing diagnosis of MV/LV distribution transformers via chemical indicators in oil. In Proceedings of the 2013 IEEE Electrical Insulation Conference (EIC), IEEE, Ottawa, ON, Canada, 2–5 June 2013; pp. 464–468.
47. Zhang, E.; Zheng, H.; Zhang, Y.; Liu, J.; Shi, Z.; Shi, K.; Zhang, C.; Shao, G.; Zhang, C.; Schwarz, H. Lifespan Model of the Relationships between Ethanol Indicator and Degree of Polymerization of Transformer Paper Insulation. *IEEE Trans. Dielectr. Electr. Insul.* **2021**, *28*, 1859–1866. [[CrossRef](#)]
48. Zhang, E.; Liu, J.; Fan, X.; Zhang, Y.; Zhang, C. Reduction Mechanism of Alcohols Contents Caused by Acids During Oil-Paper Insulation Aging. *IEEE Trans. Dielectr. Electr. Insul.* **2021**, *28*, 1867–1874. [[CrossRef](#)]
49. Wang, J.; Zhou, Y.; Liu, J.; Wang, Z.; Bai, S.; Lu, J. A new method for the aging evaluation of oil-paper insulation by n-butanol and methanol. *CSEE J. Power Energy Syst.* **2022**, *10*, 717–726.
50. Lundgaard, L.; Hansen, W.; Ingebrigtsen, S. Aging of mineral oil impregnated cellulose by acid catalysis. *IEEE Trans. Dielectr. Electr. Insul.* **2008**, *15*, 540–546. [[CrossRef](#)]
51. Yang, E.; Zheng, H.; Yang, T.; Yao, W.; Wang, Z.; Li, X.; Liu, C.; Feng, Y. Investigation on formation and solubility of formic acid, acetic acid and levulinic acid in insulating oil using COSMO-RS. *J. Mol. Liq.* **2022**, *346*, 118256. [[CrossRef](#)]
52. Cong, H.; Pan, H.; Qian, D.; Zhao, H.; Li, Q. Reviews on sulphur corrosion phenomenon of the oil–paper insulating system in mineral oil transformer. *High Volt.* **2021**, *6*, 193–209. [[CrossRef](#)]
53. Matharage, S.; Liu, Q.; Wang, Z. Generation of methanol and ethanol from inhibited mineral oil. In Proceedings of the 2017 INSUCON-13th International Electrical Insulation Conference (INSUCON), Birmingham, UK, 16–18 May 2017; pp. 1–4.
54. Emsley, A.M.; Stevens, G.C. Kinetics and mechanisms of the low-temperature degradation of cellulose. *Cellulose* **1994**, *1*, 26–56. [[CrossRef](#)]
55. Emsley, A.M. On the kinetics of degradation of cellulose. *Cellulose* **1997**, *4*, 1–5. [[CrossRef](#)]
56. Urzhumtsev, Y.S. Time-temperature superposition. *Rev. Mech. Compos. Mater.* **1975**, *11*, 57–72.
57. Heywood, R.J.; Stevens, G.C.; Ferguson, C.; Emsley, A.M. Life assessment of cable paper using slow thermal ramp methods. *Therm. Acta* **1999**, *332*, 189–195. [[CrossRef](#)]
58. Ding, H.Z.; Wang, Z.D. On the degradation evolution equations of cellulose. *Cellulose* **2008**, *15*, 205–224. [[CrossRef](#)]
59. Gillen, K.T.; Celina, M. The wear-out approach for predicting the remaining lifetime of materials. *Polym. Degrad. Stab.* **2000**, *71*, 15–30. [[CrossRef](#)]
60. Teymouri, A.; Vahidi, B. Estimation of power transformer remaining life from activation energy and pre-exponential factor in the Arrhenius equation. *Cellulose* **2019**, *26*, 9709–9720. [[CrossRef](#)]
61. Yang, L.J.; Liao, R.J.; Sun, C.X.; Zhu, M.Z. Influence of vegetable oil on the thermal aging of transformer paper and its mechanism. *IEEE Trans. Dielectr. Electr. Insul.* **2011**, *18*, 692–700. [[CrossRef](#)]
62. Mezgebo, B.; Sherif, S.S.; Fernando, N.; Senior, M.; Kordi, B. Paper Insulation Aging Estimation Using Swept-Source Optical Coherence Tomography. *IEEE Trans. Dielectr. Electr. Insul.* **2022**, *29*, 30–37. [[CrossRef](#)]
63. Liao, R.; Guo, C.; Wang, K.; Yang, L.; Grzybowski, S.; Sun, H. Investigation on thermal aging characteristics of vegetable oil-paper insulation with flowing dry air. *IEEE Trans. Dielectr. Electr. Insul.* **2013**, *20*, 1649–1658. [[CrossRef](#)]
64. Jacob, N.D.; Hassanzadeh, H.; Oliver, D.R.; Sherif, S.S.; Kordi, B. Classification of degradation in oil-impregnated cellulose insulation using texture analysis of optical microscopy images. *Electr. Power Syst. Res.* **2016**, *133*, 104–112. [[CrossRef](#)]
65. Jacob, N.D.; Kordi, B.; Sherif, S.S. Assessment of power transformer paper ageing using wavelet texture analysis of microscopy images. *IEEE Trans. Dielectr. Electr. Insul.* **2020**, *27*, 1898–1905. [[CrossRef](#)]
66. Harris, D.C. *Quantitative Chemical Analysis*, 6th ed.; W. H. Freeman and Company: New York, NY, USA, 2003.
67. Arakelian, V.G.; Fofana, I. Water in oil-filled high-voltage equipment part II: Water content as physicochemical tools for insulation condition diagnostic. *IEEE Electr. Insul. Mag.* **2007**, *23*, 15–24. [[CrossRef](#)]
68. Schärfl, W.; Xie, R.; Ren, T.; Sejfic, M.; Wenz, G.; Heisel, R.; Scherer, C.; Maskos, M.; Fischer, K.; Basché, T. Water-soluble, cyclodextrin-functionalized semiconductor nanocrystals: Preparation and pH-dependent aggregation and emission properties. *J. Lumin.* **2009**, *129*, 1428–1434. [[CrossRef](#)]
69. Liu, Y. Some consideration on the Langmuir isotherm equation. *Colloids Surf.* **2006**, *274*, 34–36. [[CrossRef](#)]
70. Langmuir, I. The constitution and fundamental properties of solids and liquids. Part I. Solids. *J. Am. Chem. Soc.* **1916**, *38*, 2221–2295. [[CrossRef](#)]
71. Chung, H.K.; Kim, W.H.; Park, J.; Cho, J.; Jeong, T.; Park, P. Application of Langmuir and Freundlich isotherms to predict adsorbate removal efficiency or required amount of adsorbent. *J. Ind. Eng. Chem.* **2015**, *28*, 241–246. [[CrossRef](#)]
72. Martin, D.; Perkasa, C.; Lelekakis, N. Measuring paper water content of transformers: A new approach using cellulose isotherms in nonequilibrium conditions. *IEEE Trans. Power Deliv.* **2013**, *28*, 1433–1439. [[CrossRef](#)]
73. Guidi, W.; Fullerton, H. Mathematical methods for prediction of moisture take-up and removal in large power transformers. *IEEE Winter Power Meet.* **1974**, *74*, 242–244.
74. Yang, L.; Zou, T.; Deng, B.; Zhang, H.; Mo, Y.; Peng, P. Assessment of oil-paper insulation aging using frequency domain spectroscopy and moisture equilibrium curves. *IEEE Access* **2019**, *7*, 45670–45678. [[CrossRef](#)]

75. Ward, B.W.; Oommen, T.V.; Thompson, J.A. Moisture estimation in transformer insulation. In Proceedings of the IEEE/PES Transformers Committee, Las Vegas, NV, USA, 24–28 October 2004.
76. Oommen, T.V. Moisture equilibrium charts for transformer insulation drying practice. *IEEE Trans. Power Appl. Syst.* **1984**, *103*, 3063–3067.
77. Wang, D.; Zhou, L.; Li, X.; Cui, Y.; Li, H.; Wang, A.; Liao, W. Effects of thermal aging on moisture equilibrium in oil-paper insulation. *IEEE Trans. Dielectr. Electr. Insul.* **2018**, *25*, 2340–2348. [[CrossRef](#)]
78. Ansari, M.A.; Martin, D.; Saha, T.K. Investigation of Distributed Moisture and Temperature Measurements in Transformers Using Fiber Optics Sensors. *IEEE Trans. Power Deliv.* **2019**, *34*, 1776–1784. [[CrossRef](#)]
79. Ansari, M.A.; Martin, D.; Saha, T.K. Advanced Online Moisture Measurements in Transformer Insulation Using Optical Sensors. *IEEE Trans. Dielectr. Electr. Insul.* **2020**, *27*, 1803–1810. [[CrossRef](#)]
80. Zhang, M.; Lei, S.; Liu, H.; Shen, Y.; Liu, J.; Shi, Y.; Jia, H.; Li, L. Research on nonlinear characteristics for frequency domain dielectric response of transformer oil-paper insulation. *Measurement* **2022**, *204*, 112103. [[CrossRef](#)]
81. Saha, T.K. Review of time-domain polarization measurements for assessing insulation condition in aged transformers. *IEEE Trans. Power Deliv.* **2003**, *18*, 1293–1301. [[CrossRef](#)]
82. Jota, P.R.S.; Islam, S.M.; Jota, F.G. Modeling the polarization spectrum in composite oil/paper insulation systems. *IEEE Trans. Dielectr. Electr. Insul.* **1999**, *6*, 145–151. [[CrossRef](#)]
83. Liu, Q.; Cai, C.; Wu, L. A novel characteristic optimization method based on combined statistical indicators and random forest for oil-paper insulation state diagnosis. *CSEE J. Power Energy Syst.* **2021**, *early access*.
84. Wolny, S. Aging degree evaluation for paper-oil insulation using the recovery voltage method. *IEEE Trans. Dielectr. Electr. Insul.* **2015**, *22*, 2455–2462. [[CrossRef](#)]
85. Martínez, M.; Pleite, J. Improvement of RVM test interpretation using a Debye equivalent circuit. *Energies* **2020**, *13*, 323. [[CrossRef](#)]
86. Yang, F.; Tang, C.; Zhou, Q.; Du, L.; Wan, H.; Chen, J. Novel characteristic quantities for determining the moisture state of Oil-impregnated cellulose insulation using the extended debye model. *IEEE Trans. Dielectr. Electr. Insul.* **2022**, *29*, 1087–1094. [[CrossRef](#)]
87. Sarkar, S.; Sharma, T.; Baral, A.; Chatterjee, B.; Dey, D.; Chakravorti, S. An expert system approach for transformer insulation diagnosis combining conventional diagnostic tests and PDC, RVM data. *IEEE Trans. Dielectr. Electr. Insul.* **2014**, *21*, 882–891. [[CrossRef](#)]
88. Saha, T.K.; Purkait, P. Investigation of an expert system for the condition assessment of transformer insulation based on dielectric response measurement. *IEEE Trans. Power Deliv.* **2004**, *19*, 1127–1134. [[CrossRef](#)]
89. Saha, T.K.; Prithwiraj, P. Investigations of temperature effects on the dielectric response measurements of transformer oil-paper insulation system. *IEEE Trans. Power Deliv.* **2007**, *23*, 252–260. [[CrossRef](#)]
90. Liao, R.; Du, Y.; Yang, L.; Gao, J. Quantitative diagnosis of moisture content in oil-paper condenser bushing insulation based on frequency domain spectroscopy and polarisation and depolarisation current. *IET Gener. Transm. Distrib.* **2017**, *11*, 1420–1426. [[CrossRef](#)]
91. Mishra, D.; Haque, N.; Baral, A.; Chakravorti, S. Assessment of interfacial charge accumulation in oil-paper interface in transformer insulation from polarization-depolarization current measurements. *IEEE Trans. Dielectr. Electr. Insul.* **2017**, *24*, 1665–1673. [[CrossRef](#)]
92. Saha, T.K.; Purkait, P.; Müller, F. Deriving an Equivalent Circuit of Transformers Insulation for Understanding the Dielectric Response Measurements. *IEEE Trans. Power Deliv.* **2005**, *20*, 149–157. [[CrossRef](#)]
93. Saha, T.K.; Purkait, P. Understanding the Impacts of Moisture and Thermal Ageing on Transformer’s Insulation by Dielectric Response and Molecular Weight Measurements. *IEEE Trans. Dielectr. Electr. Insul.* **2008**, *15*, 568–582. [[CrossRef](#)]
94. Saha, T.K.; Prithwiraj, P. Investigation of polarization and depolarization current measurements for the assessment of oil-paper insulation of aged transformers. *IEEE Trans. Dielectr. Electr. Insul.* **2004**, *11*, 144–154. [[CrossRef](#)]
95. Wei, J.; Zhang, G.; Xu, H.; Peng, H.; Wang, S.; Dong, M. Novel characteristic parameters for oil-paper insulation assessment from differential time-domain spectroscopy based on polarization and depolarization current measurement. *IEEE Trans. Dielectr. Electr. Insul.* **2011**, *18*, 1918–1928. [[CrossRef](#)]
96. Zhang, T.; Wang, S.; Zhang, C.; Siada, A.; Li, L.; Han, J.; Du, Z. Investigating a new approach for moisture assessment of transformer insulation system. *IEEE Access.* **2020**, *8*, 81458–81467. [[CrossRef](#)]
97. Zhang, D.N.; Yun, H.; Zhan, J.Y.; Sun, X.; He, W.L.; Niu, C.B.; Mu, H.B.; Zhang, G.J. Insulation Condition Diagnosis of Oil-Immersed Paper Insulation Based on Non-linear Frequency-Domain Dielectric Response. *IEEE Trans. Dielectr. Electr. Insul.* **2018**, *25*, 1980–1988. [[CrossRef](#)]
98. Liu, J.; Zhang, H.; Fan, X.; Zhang, Y.; Zhang, C. Aging evaluation for transformer oil-immersed cellulose insulation by using frequency dependent dielectric modulus technique. *Cellulose* **2021**, *28*, 2387–2401. [[CrossRef](#)]
99. Liu, J.; Fan, X.; Zhang, Y.; Zhang, C.; Wang, Z. Aging evaluation and moisture prediction of oil-immersed cellulose insulation in field transformer using frequency domain spectroscopy and aging kinetics model. *Cellulose* **2020**, *27*, 7175–7189. [[CrossRef](#)]
100. Laidler, K.J. The development of the Arrhenius equation. *J. Chem. Educ.* **1984**, *61*, 494–498. [[CrossRef](#)]
101. Zhang, M.; Liu, J.; Jia, H.; Chen, Q.; Lv, J.; Chen, X. Modelling the low-frequency electrode dielectric response based on transformer equivalent oil-paper insulation model. *IET Sci. Meas. Technol.* **2019**, *13*, 700–707. [[CrossRef](#)]

102. Boss, P.; Csepes, G.; Der, H.V.; Filippini, J.; Guuinic, P.; Gäfvert, U.; Karius, V.; Lapworth, J.; Urbani, G.; Werelius, P.; et al. Dielectric response methods for diagnostics of power transformers. *IEEE Electr. Insul. Mag.* **2003**, *19*, 12–18.
103. Liu, J.; Fan, X.; Zhang, Y.; Zheng, H.; Zhang, C. Condition prediction for oil-immersed cellulose insulation in field transformer using fitting fingerprint database. *IEEE Trans. Dielectr. Electr. Insul.* **2020**, *27*, 279–287. [[CrossRef](#)]
104. Jonscher, A.K. Dielectric relaxation in solids. *J. Phys. D Appl. Phys.* **1999**, *32*, 57–70. [[CrossRef](#)]
105. Das, A.K.; Dalai, S.; Chatterjee, B. A Novel Approach to Estimate the Quantity of Ingressed Moisture Content Inside Metal Oxide Surge Arrester Using Dielectric Modulus Technique. *IEEE Trans. Dielectr. Electr. Insul.* **2021**, *28*, 2178–2185. [[CrossRef](#)]
106. Liu, J.; Fan, X.; Zhang, Y.; Lai, B.; Jiao, J. Analysis of low-frequency polarisation behaviour for oil-paper insulation using logarithmic-derivative spectroscopy. *High Volt.* **2021**, *6*, 460–469. [[CrossRef](#)]
107. Liu, J.; Fan, X.; Zhang, Y.; Zheng, H.; Zhu, M. Quantitative evaluation for moisture content of cellulose insulation material in paper/oil system based on frequency dielectric modulus technique. *Cellulose* **2020**, *27*, 2343–2356. [[CrossRef](#)]
108. Yang, F.; Du, L.; Yang, L.; Wei, C.; Wang, Y.; Ran, L.; He, P. A parameterization approach for the dielectric response model of oil paper insulation using FDS measurements. *Energies* **2018**, *11*, 622. [[CrossRef](#)]
109. Sumranbumrung, R.; Khunkitti, P.; Siritaratiwat, A.; Kruesubthaworn, A. Characterization Model of Dielectric Properties of Cane Sugar Solution Over 0.5–14 GHz. *IEEE Trans. Instrum. Meas.* **2021**, *70*, 8003908. [[CrossRef](#)]
110. Morsalin, S.; Phung, B.T. Modeling of Dielectric Dissipation Factor Measurement for XLPE Cable Based on Davidson-Cole Model. *IEEE Trans. Dielectr. Electr. Insul.* **2019**, *26*, 1018–1026. [[CrossRef](#)]
111. Das, A.K.; Haque, N.; Pradhan, A.K.; Dalai, S.; Chatterjee, B.; Mukherjee, A. Estimation of Moisture Content in XLPE Insulation in Medium Voltage Cable by Frequency Domain Spectroscopy. *IEEE Trans. Dielectr. Electr. Insul.* **2020**, *27*, 1811–1819. [[CrossRef](#)]
112. Xia, G.; Wu, G.; Gao, B.; Yin, H.; Yang, F. A new method for evaluating moisture content and aging degree of transformer oil-paper insulation based on frequency domain spectroscopy. *Energies* **2017**, *10*, 1195. [[CrossRef](#)]
113. Zhou, L.; Wang, D.; Guo, L.; Wang, L.; Jiang, J.; Liao, W. FDS analysis for multilayer insulation paper with different aging status in traction transformer of high-speed railway. *IEEE Trans. Dielectr. Electr. Insul.* **2017**, *24*, 3236–3244. [[CrossRef](#)]
114. Hao, J.; Liao, R.; Chen, G.; Ma, Z.; Yang, L. Quantitative analysis ageing status of natural ester-paper insulation and mineral oil-paper insulation by polarization/depolarization current. *IEEE Trans. Dielectr. Electr. Insul.* **2012**, *19*, 188–199.
115. Liao, R.; Liu, J.; Yang, L.; Gao, J.; Zhang, Y.; Lv, Y.; Zheng, H. Understanding and analysis on frequency dielectric parameter for quantitative diagnosis of moisture content in paper–oil insulation system. *IET Electr. Power Appl.* **2015**, *9*, 213–222. [[CrossRef](#)]
116. Gao, J.; Yang, L.; Wang, Y.; Qi, C.; Hao, J.; Liu, J. Quantitative evaluation of ageing condition of oil-paper insulation using frequency domain characteristic extracted from modified cole-cole model. *IEEE Trans. Dielectr. Electr. Insul.* **2015**, *22*, 2694–2702. [[CrossRef](#)]
117. Zhang, M.; Liu, J.; Yin, M.; Jia, H.; Lv, J. Assessment on oil-paper insulation aging of transformer based on dielectric response model. *Electr. Power Compon. Syst.* **2019**, *47*, 1145–1155. [[CrossRef](#)]
118. Yang, D.; Chen, W.; Wan, F.; Zhou, Y.; Wang, J. Identification of the aging stage of transformer oil-paper insulation via Raman spectroscopic characteristics. *IEEE Trans. Dielectr. Electr. Insul.* **2020**, *27*, 1770–1777. [[CrossRef](#)]
119. Zhou, Y.; Chen, W.; Yang, D.; Zhang, R. Raman spectrum characteristics and aging diagnosis of oil-paper insulation with different oil-paper ratios. *IEEE Trans. Dielectr. Electr. Insul.* **2020**, *27*, 1587–1594. [[CrossRef](#)]
120. Ashkezari, A.D.; Ma, H.; Saha, T.K.; Ekanayake, C. Application of fuzzy support vector machine for determining the health index of the insulation system of in-service power transformers. *IEEE Trans. Dielectr. Electr. Insul.* **2013**, *20*, 965–973. [[CrossRef](#)]
121. Liu, J.; Fan, X.; Zhang, C.; Lai, C.; Zhang, Y.; Zheng, H.; Lai, L.; Zhang, E. Moisture diagnosis of transformer oil-immersed insulation with intelligent technique and frequency-domain spectroscopy. *IEEE Trans. Ind. Inform.* **2020**, *17*, 4624–4634. [[CrossRef](#)]
122. Cui, Y.; Ma, H.; Saha, T. Improvement of power transformer insulation diagnosis using oil characteristics data preprocessed by SMOTEBoost technique. *IEEE Trans. Dielectr. Electr. Insul.* **2014**, *21*, 2363–2373. [[CrossRef](#)]
123. Li, Y.; Zhang, Y.; Zhang, W.B.; Xu, Y.; Zhang, G. Comparative study of partial least squares and neural network models of near-infrared spectroscopy for aging condition assessment of insulating paper. *Meas. Sci. Technol.* **2020**, *31*, 045501. [[CrossRef](#)]
124. Fan, X.; Liu, J.; Lai, B.; Zhang, Y.; Zhang, C. FDS measurement-based moisture estimation model for transformer oil-paper insulation including the aging effect. *IEEE Trans. Instrum. Meas.* **2021**, *70*, 1–10. [[CrossRef](#)]
125. Yutthago, P. Effective Oil-Immersed Paper Insulation Condition Assessment of Power Transformers. *SSRN* **2022**. [[CrossRef](#)]
126. Xie, Y.; Ruan, J.; Shi, Y.; Jin, S.; Tian, Y.; Zhu, L. Inversion detection method for resistivity of oil-immersed paper in transformer. *IEEE Trans. Power Deliv.* **2019**, *34*, 1757–1765. [[CrossRef](#)]
127. Yang, Z.; Zhou, Q.; Wu, X.; Zhao, Z.; Tang, C.; Chen, W. Detection of water content in transformer oil using multi frequency ultrasonic with PCA-GA-BPNN. *Energies* **2019**, *12*, 1379. [[CrossRef](#)]
128. Liu, J.; Ding, Z.; Fan, X.; Geng, C.; Song, B.; Wang, Q.; Zhang, Y. A BPNN model-based AdaBoost algorithm for estimating inside moisture of oil–paper insulation of power transformer. *IEEE Trans. Dielectr. Electr. Insul.* **2022**, *29*, 614–622. [[CrossRef](#)]
129. Zhang, M.; Li, L.; Liu, H.; Jia, H.; Meng, F. Method for quantitative assessment of transformer oil-paper insulation non-uniform ageing parameters based on frequency domain dielectric response. *IET Sci. Meas. Technol.* **2022**, *16*, 118–129. [[CrossRef](#)]
130. Baral, A.; Chakravorti, S. A modified Maxwell model for characterization of relaxation processes within insulation system having non-uniform aging due to temperature gradient. *IEEE Trans. Dielectr. Electr. Insul.* **2013**, *20*, 524–534. [[CrossRef](#)]
131. Jalbert, J.; Lessard, M.C.; Ryadi, M. Cellulose chemical markers in transformer oil insulation Part 1: Temperature correction factors. *IEEE Trans. Dielectr. Electr. Insul.* **2013**, *20*, 2287–2291. [[CrossRef](#)]

132. Zhang, E.; Liu, J.; Song, B.; Zhang, H.; Fan, X.; Zhang, Y.; Fu, Q. Influence of Operational Defects and Hotspot Temperature on Methanol Concentration in Transformer Oil. *IEEE Trans. Power Deliv.* **2022**, *38*, 1859–1867. [[CrossRef](#)]
133. Sun, W.; Yang, L.; Zare, F.; Lin, Y.; Cheng, Z. Improved method for aging assessment of winding hot-spot insulation of transformer based on the 2-FAL concentration in oil. *Inter J. Electr. Power Energy Syst.* **2019**, *112*, 191–198. [[CrossRef](#)]
134. Zhou, L.; Wang, D.; Cui, Y.; Zhang, L.; Wang, L.; Guo, L. A method for diagnosing the state of insulation paper in traction transformer based on FDS test and CS-DQ algorithm. *IEEE Trans. Transport. Electrification.* **2020**, *7*, 91–103. [[CrossRef](#)]
135. Zhang, Y.; Yang, L.; Su, Z.; Wei, W.; Dong, C.; Huang, Z.; Hua, J. Time Domain Dielectric Response Characteristics of Oil-Immersed Paper Bushings Under Radial Nonuniform Moisture. *IEEE Trans. Dielectr. Electr. Insul.* **2023**, *31*, 1079–1086. [[CrossRef](#)]
136. Liu, J.; Sun, T.; Fan, X.; Zhang, Y.; Lai, B. A modified simulation model for predicting the FDS of transformer oil-paper insulation under nonuniform aging. *IEEE Trans. Instrum. Meas.* **2021**, *70*, 1–9. [[CrossRef](#)]
137. Liu, J.; Wang, Q.; Fan, X.; Zhang, Y.; Goh, H.H. Effects of Temperature Gradient Induced Aging and Moisture Distribution on Dielectric Response Measurement for Transformer Insulation. *IEEE Trans. Instrum. Meas.* **2022**, *71*, 1–10. [[CrossRef](#)]
138. Baral, A.; Chakravorti, S. Condition assessment of cellulosic part in power transformer insulation using transfer function zero of modified Debye model. *IEEE Trans. Dielectr. Electr. Insul.* **2014**, *21*, 2028–2036. [[CrossRef](#)]
139. Fan, X.; Liu, J.; Goh, H.H.; Zhang, Y.; Zhang, C.; Rahman, S. Acquisition of FDS for oil-immersed insulation at transformer hotspot region based on multiconstraint NSGA model. *IEEE Trans. Ind. Electron.* **2022**, *69*, 13625–13635. [[CrossRef](#)]
140. Islam, M.M.; Lee, G.; Hettiwatte, S.N. A review of condition monitoring techniques and diagnostic tests for lifetime estimation of power transformers. *Electr. Eng.* **2018**, *100*, 581–605. [[CrossRef](#)]
141. Hosier, I.L.; Koilraj, J.E.A.; Vaughan, A.S. Effect of aging on the physical, chemical and dielectric properties of dodecylbenzene. *IEEE Trans. Dielectr. Electr. Insul.* **2016**, *23*, 3389–3396. [[CrossRef](#)]
142. Jadav, R.B.; Ekanayake, C.; Saha, T.K. Understanding the impact of moisture and ageing of transformer insulation on frequency domain spectroscopy. *IEEE Trans. Dielectr. Electr. Insul.* **2014**, *21*, 369–379. [[CrossRef](#)]
143. Teymouri, A.; Vahidi, B.; Wielen, P. A novel life management model consists of chemical aging model and electrical-thermal aging model for power transformers using a new activation energy calculation method. *Cellulose* **2022**, *29*, 4455–4473. [[CrossRef](#)]
144. Deng, Y.; Fan, X.; Luo, H.; Wang, Y.; Wu, K.; Liang, F.; Li, C. Impact of Air Gap Defects on the Electrical and Mechanical Properties of a 320 kV Direct Current Gas Insulated Transmission Line Spacer. *Energies* **2023**, *16*, 4006. [[CrossRef](#)]

Disclaimer/Publisher’s Note: The statements, opinions and data contained in all publications are solely those of the individual author(s) and contributor(s) and not of MDPI and/or the editor(s). MDPI and/or the editor(s) disclaim responsibility for any injury to people or property resulting from any ideas, methods, instructions or products referred to in the content.